

This is a repository copy of *The role of default mode network in semantic cue integration*.

White Rose Research Online URL for this paper:

<https://eprints.whiterose.ac.uk/162119/>

Version: Accepted Version

Article:

Lanzoni, Lucilla, Ravasio, Daniela, Thompson, Hannah Elizabeth et al. (4 more authors) (2020) The role of default mode network in semantic cue integration. *Neuroimage*. 117019. ISSN 1053-8119

<https://doi.org/10.1016/j.neuroimage.2020.117019>

Reuse

Items deposited in White Rose Research Online are protected by copyright, with all rights reserved unless indicated otherwise. They may be downloaded and/or printed for private study, or other acts as permitted by national copyright laws. The publisher or other rights holders may allow further reproduction and re-use of the full text version. This is indicated by the licence information on the White Rose Research Online record for the item.

Takedown

If you consider content in White Rose Research Online to be in breach of UK law, please notify us by emailing eprints@whiterose.ac.uk including the URL of the record and the reason for the withdrawal request.

The role of default mode network in semantic cue integration

Lucilla Lanzoni¹, Daniela Ravasio², Hannah Thompson³, Deniz Vatansever⁴, Daniel Margulies⁵, Jonathan Smallwood¹ & Elizabeth Jefferies¹

1 Department of Psychology, University of York, UK

2 Department of Psychological Sciences, University of Bergamo, Italy

3 School of Psychology, University of Surrey, UK

4 Institute of Science and Technology for Brain-inspired Intelligence, Fudan University, Shanghai, PR China.

5 Institute du Cerveau et de la Moelle épinière (ICM), Paris, France

* Corresponding author1: Lucilla Lanzoni

Email: lucilla.lanzoni@york.ac.uk

Phone: 01904 322928

University of York, Heslington, York

YO10 5DD

* Corresponding author2: Elizabeth Jefferies

Email: beth.jefferies@york.ac.uk

Phone: 01904 324368

University of York, Heslington, York

YO10 5DD

UK

Funding

The study was supported by a grant from the Stroke Association [R1425201] and a grant from the European Research Council [FLEXSEM – 771863] awarded to E.J.

Declarations of interest: none

1 **ABSTRACT**

2 Recent accounts of large-scale cortical organisation suggest that the default mode network
3 (DMN) is positioned at the top of a principal gradient, reflecting the separation between
4 heteromodal and unimodal sensory-motor regions in patterns of connectivity and in geodesic
5 distance along the cortical surface (Margulies et al., 2016). This isolation of DMN from external
6 inputs might allow the integration of disparate sources of information that can constrain
7 subsequent cognition. We tested this hypothesis by manipulating the degree to which
8 semantic decisions for ambiguous words (e.g. JAM) were constrained by preceding visual cues
9 depicting relevant spatial contexts (e.g. SUPERMARKET or ROAD) and/or facial emotions (e.g. HAPPY
10 vs. FRUSTRATED). We contrasted (i) the effects of a single preceding cue with a no-cue condition
11 employing scrambled images, and (ii) convergent spatial and emotion cues with single cues.
12 Single cues elicited stronger activation in the multiple demand network relative to no cues,
13 consistent with the requirement to maintain information in working memory. The availability
14 of two convergent cues elicited stronger activation within DMN regions (bilateral angular
15 gyrus, middle temporal gyrus, medial prefrontal cortex, and posterior cingulate), even though
16 behavioural performance was unchanged by cueing – consequently task difficulty is unlikely to
17 account for the observed differences in brain activation. A regions-of-interest analysis along
18 the unimodal-to-heteromodal principal gradient revealed maximal activation for the
19 convergent cue condition at the heteromodal end, corresponding to the DMN. Our findings
20 are consistent with the view that regions of DMN support states of information integration
21 that constrain ongoing cognition and provide a framework for understanding the location of
22 these effects at the heteromodal end of the principal gradient.

23 **Keywords:** default mode, integration, principal gradient, semantics, cueing

24

25 1. INTRODUCTION

26 The context in which we encounter concepts in our daily life influences the manner in
27 which we think about them. Hearing the word *jam* at the kitchen table, for example, one might
28 activate a number of concepts related to food, its taste and emotional valence. The same word
29 *jam* on the traffic news, however, might bring up very different thoughts and emotions.
30 Although studies have manipulated sentence contexts to constrain the interpretation of
31 ambiguous words (e.g. Noonan et al., 2010; Rodd et al., 2016; Rodd et al., 2005; Rodd et al.,
32 2004; Rodd et al., 2013; Vitello & Rodd, 2015), cues beyond language have rarely been
33 employed (for an exception see Lanzoni et al., 2019). Consequently, relatively little is known
34 about how non-verbal cues, such as spatial location and affect, constrain meaning retrieval or
35 the neural mechanisms that underlie this effect. The current study addressed this issue by
36 manipulating the availability of spatial and facial emotion cues prior to semantic decisions
37 about ambiguous words.

38 Contemporary models of semantic cognition suggest that retrieval is supported by a
39 dynamic interplay of conceptual knowledge with retrieval processes (Hoffman et al., 2018;
40 Jefferies, 2013; Lambon Ralph et al., 2016). Conceptual representations are rich and comprise
41 features from multiple sensory modalities (e.g. an apple is a *sweet* fruit, with a *rounded* shape
42 and a *smooth hard* surface which is often *red, yellow* or *green*). According to the Hub and Spoke
43 model of conceptual representation, the ventrolateral anterior temporal lobe (ATL) ‘hub’
44 integrates features encoded in sensory-motor cortical ‘spokes’ to generate coherent
45 representations – e.g. our concept ‘apple’ (Chiou & Lambon Ralph, 2019; Patterson et al., 2007;
46 Lambon Ralph et al., 2016). However, hub and spoke representations are not sufficient to
47 support *flexible* semantic cognition; we also dynamically vary the aspects of knowledge that
48 we retrieve about concepts depending on the context. Semantic processing may draw on
49 different large-scale networks depending on whether retrieval is usefully constrained or
50 miscued by the context.

51 In line with this view, semantic sites have been shown to overlap with distinct large-
52 scale networks that are recruited differentially depending on the task demands. When non-
53 dominant associations are required by a task, or the prior context is unhelpful, a ‘semantic
54 control network’ is recruited (including left inferior frontal gyrus and posterior middle temporal
55 gyrus), which may shape retrieval to suit the circumstances (Badre & Wagner, 2005, 2006;

56 Davey et al., 2016; Hallam et al., 2016; Krieger-Redwood et al., 2015; Noonan et al., 2013;
57 Whitney et al., 2011). In contrast, other key sites for semantic cognition, such as lateral ATL
58 and angular gyrus (AG), have patterns of intrinsic connectivity that are partially overlapping
59 with aspects of the Default Mode Network (DMN) (Davey et al., 2016; Humphreys & Lambon
60 Ralph, 2014; Jackson et al., 2016; Seghier et al., 2010). The role of DMN regions in semantic
61 cognition remains controversial: a meta-analysis by Binder and colleagues (2009) found peak
62 activation for semantic tasks in AG, while other researchers have characterized AG as a task-
63 negative region which deactivates across semantic and non-semantic tasks (Humphreys et al.,
64 2015; Humphreys & Lambon Ralph, 2014; Mollo et al., 2017). DMN regions, including AG,
65 typically show anti-correlation with task-positive regions within the multiple demand network
66 (MDN; Blank et al., 2014; Davey et al., 2016; Fox et al., 2005). Nevertheless, TMS studies have
67 shown that AG plays a critical role in the efficient retrieval of dominant aspects of knowledge
68 (Davey et al., 2015). There are also demonstrations of a role for the DMN in semantic retrieval
69 even when tasks are relatively hard. For example, Murphy et al. (2018) found greater DMN
70 recruitment both when participants made judgements based on their memory of preceding
71 trials (as opposed to stimuli present on the screen), and when the decisions involved semantic
72 categories as opposed to perceptual features.

73 Recent studies have suggested that semantic regions allied to DMN, including AG,
74 support the combination of concepts into meaningful and more complex representations (e.g.
75 Price et al., 2015; for a review see Pylkkänen, 2019). These regions show a stronger response
76 when coherent conceptual combinations or heteromodal features are presented (Bemis &
77 Pylkkänen, 2011; Price et al., 2015; 2016; Pylkkänen, 2019; Teige et al., 2018; 2019). The
78 suggested critical role of the DMN in conceptual integration fits well with the observation that
79 the DMN lies at the top of a cortical hierarchy. Through decomposition of resting-state
80 connectivity, Margulies et al. (2016) identified a principal gradient of macroscale organization,
81 anchored at one end by sensory regions and at the other end by heteromodal cortex,
82 corresponding to the DMN. This separation of DMN from unimodal cortex in intrinsic
83 connectivity relates to geodesic distance – DMN sites are located relatively far away from
84 primary sensory-motor cortex along the cortical surface (Margulies et al., 2016). Greater
85 distance along the gradient might allow the brain to support forms of cognition that rely on
86 memory, as opposed to information in the external environment (Murphy et al., 2019).

87 Distance might also support increasing levels of abstraction from sensory-motor features,
88 allowing the formation of heteromodal conceptual representations from the integration of
89 these diverse sources of information (Buckner & Krienen, 2013; Mesulam, 1998; Patterson et
90 al., 2007; Smallwood, 2013). In line with this idea, default mode regions might show a greater
91 response in semantic tasks when multiple aspects of a concept are activated during retrieval.

92 In the present study, we tested the view that semantically-relevant regions within the
93 DMN, in particular AG, contribute to conceptual integration. We adopted a paradigm recently
94 developed to assess the impact of non-verbal cues in patients with semantic aphasia, who have
95 deficits of semantic control (Lanzoni et al., 2019). Participants were shown 0, 1 or 2 cues that
96 were relevant to the subsequent interpretation of an ambiguous word: they saw photographs
97 of spatial contexts, facial emotions or scrambled meaningless versions of these cues. The cues
98 alone were not sufficient to prime the concepts and did not influence behavioural performance
99 (for example, SUPERMARKET and HAPPY FACE can be linked in many ways and do not strongly
100 anticipate JAM AS FOOD). Nevertheless, the cues allowed the subsequent semantic decisions to
101 unfold in a conceptually-rich context. If semantic integration occurs in the DMN, comparing
102 semantic decisions in the context of multiple convergent cues as opposed to single cues should
103 reveal increased activation within this network and in particular in AG – even though semantic
104 decisions to ambiguous words are relatively cognitively effortful. In contrast, brain regions that
105 selectively encode and maintain semantic cue information *prior* to integration should be
106 spatially distinct from DMN: the neural basis of cue maintenance might be maximally revealed
107 by a contrast of single cue over no cue trials (as this contrasts situations where there are
108 working memory demands versus no requirement to maintain information). MDN is a
109 candidate network for attentional and working memory components of the cueing task, since
110 this network is associated with executively demanding aspects of cognition, including working
111 memory and the maintenance of task rules, across domains (e.g. Owen et al., 2005; Naghavi &
112 Nyberg, 2005; Dosenbach et al., 2006). For example, a study by Dumontheil et al. (2010) found
113 activation in several parts of MDN during the presentation of task instructions, which might
114 reflect the creation of a task-model or framework for ongoing cognition.

115 Additionally, we predicted that the effect of conceptual integration but not cue load
116 would be located at the heteromodal end of the principal gradient (Margulies et al., 2016),
117 providing a framework for understanding *why* information integration effects occur where

118 they do within the cortex: these effects should be greatest at the DMN apex of the gradient,
119 which is maximally separated (both in terms of physical distance and in connectivity terms)
120 from unimodal input or ‘spoke’ regions associated with processing specific features. In contrast
121 to our standard whole-brain cluster-corrected contrasts, the focus of this analysis was not on
122 the functional contribution of specific regions, such as AG, to cue integration, but instead on
123 whole-brain patterns that include similar functional transitions between heteromodal and
124 unimodal cortex in distant cortical regions.

125

126 2. MATERIALS AND METHODS

127 2.1 Participants

128 Twenty-seven healthy right-handed native English-speaking participants with normal or
129 corrected-to-normal vision were recruited from the University of York (9 males, mean age 21.5,
130 SD 2.9, range 19-30). Participants received monetary compensation or course credits. One
131 dataset was excluded due to technical problems that resulted in no behavioural responses
132 being recorded, leaving 26 subjects in the final sample. In a subsequent analysis we examined
133 resting-state fMRI data from 86 participants (22 males; mean age 20.3, range 18–32 years),
134 twelve of whom were also in the main sample. The research was approved by the York
135 Neuroimaging Centre Ethics Committee and participants provided written informed consent.

136 2.2 Materials

137 The cueing paradigm, adapted from Lanzoni et al. (2019), presented pictures of facial
138 expressions and spatial locations prior to semantic judgements about ambiguous words. The
139 stimuli are available on the Open Science Framework (<https://osf.io/wp6a7/>)¹. Thirty English
140 homonyms were selected from the Free Association Norms of Twilley et al. (1994), and the
141 Gawlick-Greender & Woltz norms (1994). We chose items where the different interpretations
142 were associated with different facial expressions (e.g. JAM with *traffic* is associated with
143 frustration while JAM with *strawberry* is associated with pleasure). We also chose items where
144 different interpretations were associated with different locations (e.g. a motorway for *traffic*
145 JAM and a supermarket for *strawberry* JAM). We then generated four target words for each

¹ The images of spatial locations are not included in the collection due to potential copyright restrictions.

146 probe, two for each interpretation. This resulted in 120 probe-target pairs. For instance, the
147 probe JAM appeared in four trials, twice paired with a target referring to *traffic* (JAM-horn or
148 JAM-delay) and twice paired with a target referring to the alternative interpretation (JAM-spoon
149 or JAM-bread). Although we did not manipulate the difference in frequency between the two
150 alternative meanings, one interpretation of the homonym was dominant over the other (i.e.,
151 a larger proportion of subjects generated words linked to that interpretation, as reported in
152 Twilley et al., 1994). Dominance was controlled by counterbalancing the assignment of each
153 interpretation to the different experimental conditions across participants. For each
154 combination of probes and targets, two unrelated distractors were selected. Latent Semantic
155 Analysis (as implemented in lsa.colorado.edu) was used to calculate the similarity in semantic
156 space between the probe and the targets vs. probe and distractors (parameters used: space –
157 General reading up to 1st year college, comparison type - term to term, number of factors –
158 maximum). This confirmed that the strength of the relationship between probe and distractor
159 ($M = .08$, $SD = .04$) was significantly weaker compared to the association between probe and
160 target ($M = .22$, $SD = .10$; $t(29) = 7.17$, $p < .001$). Distractors and target words were matched
161 for lexical frequency (SUBTLEX-UK database, van Heuven et al., 2014; $t = .89$, $p = .380$), word
162 length ($t = -1.44$, $p = .154$), and concreteness (Brysbaert et al., 2014; $t = .58$, $p = .564$).

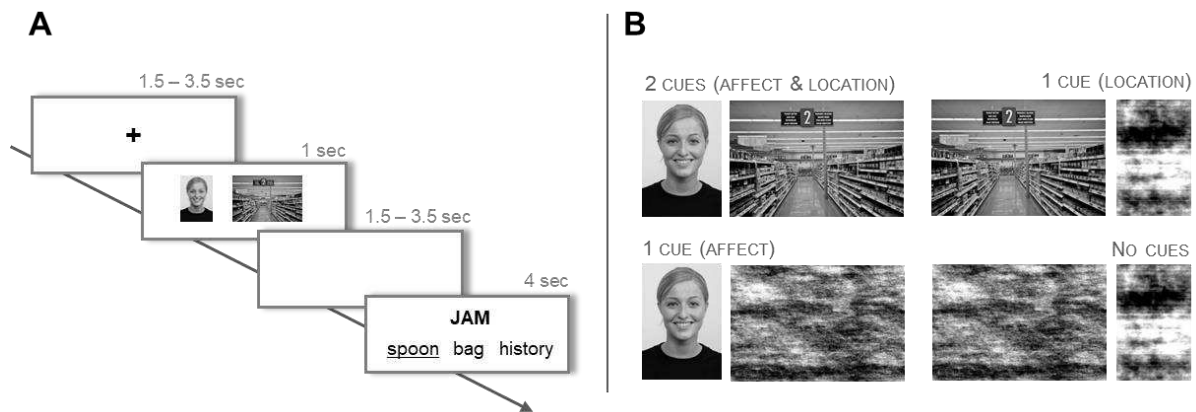
163 Pictures of facial emotional expressions and spatial locations were used to prime the
164 relevant meaning of the homonym. Each picture was used only once across the entire
165 experiment, making it impossible for participants to predict the following probe word on the
166 basis of the cue. Images of facial expressions were chosen from the Radboud Faces Database
167 (Langner et al., 2010) and included eight basic emotions: happy, angry, sad, disgusted,
168 contemptuous, surprised, neutral, fearful. In selecting the affect cues we ensured that the
169 same face from the Radboud Database would not be presented in the same emotional
170 expression in other trials. Therefore, for trials that required the same emotional expression we
171 chose different actors. Pictures of spatial contexts were downloaded from Google images.

172 The emotion and location cues could appear together in the same trial (2 cues
173 condition), they could be presented alone (1 cue affect or location conditions), in which case
174 they were paired with one meaningless scrambled image, or two scrambled images were
175 provided (no-cue condition). Images were converted to greyscale, matched for luminance and
176 scrambled using the SHINE toolbox (Willenbockel et al., 2010). Images were also brought to a

177 fixed dimension (600 x 400 pixels for location and 260 x 400 for affect cues) using Matlab (The
178 MathWorks Inc., Natick, MA, US). Figure 1B shows the 4 cue conditions, which were used to
179 examine three levels of constraint on semantic retrieval. The location of the emotion and
180 location cues (to the left or right of the screen) was counterbalanced within each run. Finally,
181 to ensure that people could not make their decisions based only on the cue, in each trial one
182 of the distractors was related to either the emotional cue or the visuo-spatial cue presented
183 before the semantic task (in Figure 1A, the distractor 'bag' is related to the location cue –
184 supermarket). The assignment of the emotion-related and location-related distractors to the
185 different conditions was counterbalanced within participants, such that each probe appeared
186 twice with an emotion-related distractor and twice with a location-related distractor.

187 **2.3 Procedure**

188 The MRI session included a high-resolution structural scan, a FLAIR sequence and four
189 functional runs of approximately nine minutes each. Each trial started with a fixation cross of
190 random duration between 1500 and 3000ms (Figure 1A). Two cue pictures or scrambled cues
191 were then presented for 1s, followed by another jittered inter-stimulus interval (ISI: 1500 –
192 3000ms). Participants were asked to pay attention to the cues, and they were told that these
193 would be helpful images on some trials, and meaningless images on other trials. Next, four
194 words appeared on screen – a probe word at the top and three response options underneath,
195 marking the start of the semantic task. Participants were asked to decide which of the three
196 options had the strongest semantic relationship to the probe, and they were encouraged to
197 make the semantic decision based on the words and not on the previously seen images.
198 Although the time to respond was fixed (4s), participants were asked to respond as quickly and
199 accurately as possible. Each of the 30 probes was presented once within each run, resulting in
200 30 semantic trials. The order of presentation was randomized and stimuli were
201 counterbalanced so that, across all participants, each probe-target combination appeared in
202 all four cue conditions. Each run had a total of eight non-semantic trials, in which words were
203 replaced with strings of the letter 'X' matched in length to the words. Here the task was to
204 press any key. The scrambled images used in non-semantic trials were created equally often
205 from face and location photos. Two null trials were also included to improve task modelling.
206 During null trials participants saw a blank screen for the same duration of 4 seconds.



207

208 Figure 1. A. After an initial fixation cross (1500 – 3000 ms), participants were presented with cue images for 1000
 209 ms, before moving to a blank screen (1500 – 3000 ms). Following that, a probe word was presented above a target
 210 and two unrelated distracters, triggering the onset of the decision-making period. The probe and choices
 211 remained visible for a fixed interval of 4000 ms. B. The four levels of the variable cue are shown.

212 **2.4 fMRI acquisition**

213 Whole brain fMRI data acquisition was performed using a GE 3 Tesla HDx Excite MRI scanner.
 214 Structural MRI data acquisition in all participants was based on a T1-weighted 3D fast spoiled
 215 gradient echo sequence (TR = 7.8ms, TE = minimum full, flip-angle = 20°, matrix size = 256x256,
 216 176 slices, voxel size = 1.13x1.13x1 mm). A gradient-echo EPI sequence was used to collect
 217 functional data from 60 interleaved bottom-up axial slices aligned with the temporal lobe (TR
 218 = 3s, TE = 18.9 ms, FOV = 192x192x180 mm, matrix size = 64x64, slice thickness = 3mm, slice-
 219 gap = 3mm, voxel size = 3x3x3 mm³, flip-angle = 90°). An intermediary FLAIR scan with the same
 220 orientation as the functional scans was collected to improve the co-registration between
 221 subject-specific structural and functional scans.

222 **2.5 Data preprocessing**

223 **2.5.1 Behavioural pre-processing and analysis**

224 We examined accuracy, median response time (RT), RT variability and response efficiency in
 225 separate repeated-measures ANOVAs to characterise differences in performance across the 4
 226 semantic conditions (0 cues, 1 cue affect, 1 cue location, 2 cues: affect and location). One
 227 keypress was not recorded for two participants and these missing RT values were replaced with
 228 the group median for that condition. Response efficiency scores were used to account for any
 229 speed-accuracy trade-offs: the median RT for correct responses for each subject in each

230 condition was divided by the mean accuracy in the same condition (Townsend & Ashby, 1983).
231 We also examined trial-to-trial variability, using the standard deviation of RT for each
232 participant in each condition.

233 *2.5.2 MRI data pre-processing*

234 fMRI data processing was carried out using FEAT (fMRI Expert Analysis Tool) Version 6.0, part
235 of FSL (FMRIB's Software Library, www.fmrib.ox.ac.uk/fsl). Registration of the high resolution
236 structural to standard space (Montreal Neurological Institute – MNI) was carried out using
237 FLIRT (Jenkinson et al., 2002; Jenkinson & Smith, 2001). Pre-processing of the functional image
238 included motion correction using MCFLIRT (Jenkinson et al., 2002), slice-timing correction
239 using Fourier-space time-series phase-shifting (interleaved), non-brain removal using BET
240 (Smith, 2002), spatial smoothing using a Gaussian kernel of FWHM 5mm, grand-mean intensity
241 normalisation of the entire 4D dataset by a single multiplicative factor, and high-pass temporal
242 filtering (Gaussian-weighted least-squares straight line fitting, with $\sigma=50.0s$).

243 *2.6 Statistical modelling*

244 Pre-processed time series were modelled using a general linear model using FILM correcting
245 for local autocorrelation (Woolrich et al., 2001). We used an event-related design. We built
246 two separate models, a *semantic decision model* to look for brain changes during semantic
247 decisions following different levels of cueing, and a *cue model* to identify brain regions that
248 responded to the presentation of the cues. Our key focus was on the semantic decision model,
249 since this established whether specific networks or gradient patterns were associated with
250 making semantic decisions in the context of single or convergent cues. The *semantic decision*
251 *model* included 8 EVs: correct semantic decisions following each of the 4 experimental
252 conditions (0 cues, 1 cue affect, 1 cue location, 2 cues), non-semantic trials where strings of
253 “Xs” were presented, remaining time in the semantic trials after making a decision before the
254 start of a new trial, cue presentation period (combining all the cue presentation events,
255 irrespective of the cue condition), and incorrect semantic trials. Given that this model revealed
256 two distinct networks associated with the maintenance of single cues as opposed to no cues,
257 and the convergence of multiple cues vs. a single cue, we then elected to examine the response
258 during cue presentation in a second stage of the analysis. The *cue model* included 6 Explanatory
259 Variables (EVs) corresponding to the 4 cue conditions (0 cue condition containing scrambled

260 images, 1 face cue + scrambled image, 1 location cue + scrambled image, 2 cues: face and
261 location), the semantic task, and the non-semantic task. The cue model established whether
262 MDN regions responding to one > no cues showed load-dependent effects during cue
263 encoding, consistent with increasing working memory demands of cue maintenance. However,
264 it is important to acknowledge that the study was not designed to examine the cue phase in
265 this fashion, and there are limitations of this exploratory analysis – in particular, the study did
266 not de-confound the order of the cue presentation and semantic decision phases, as cues were
267 always followed by the semantic task (albeit separated by a jittered interval; see limitations in
268 Discussion). All regressors were modelled using a variable epoch model, with the appearance
269 of the words (or the cue images, for the *cue model*) as the start of the event and the response
270 time (or the duration of the cue presentation) as the duration of the event. Convolution of the
271 hemodynamic response was achieved using a Gamma function (phase = 0, SD = 3, mean = 6).
272 Temporal derivatives were added to each regressor. Nuisance regressors included standard +
273 extended motion parameters. Absolute framewise displacement ranged from 0.05 mm to 0.64,
274 with a mean value of 0.21 mm across the 4 runs.

275 We then averaged contrast estimates over the four runs within each subject using a fixed
276 effects model, by forcing the random effects variance to zero in FLAME (FMRIB's Local Analysis
277 of Mixed Effects) (Beckmann et al., 2003; Woolrich, 2008; Woolrich et al., 2004). The group
278 analysis was carried out using FLAME (FMRIB's Local Analysis of Mixed Effects) stage 1
279 (Beckmann et al., 2003; Woolrich, 2008; Woolrich et al., 2004). Z (Gaussianised T/F) statistic
280 images were thresholded using clusters determined by $z > 3.1$ and a (corrected) cluster
281 significance threshold of $p = 0.05$ (Worsley, 2001). Our analysis focused on the comparison
282 between semantic decisions which followed different levels of cue: 2 cues > 1 cue (collapsing
283 across emotion and location cues) and 1 cue > 0 cues.

284 Cognitive decoding of the main contrasts of interest was performed in Neurosynth, an
285 automated meta-analysis tool (Yarkoni et al., 2011). Unthresholded z maps were uploaded to
286 Neurosynth to obtain psychological terms associated with the patterns of activation in our
287 results. Where multiple terms had the same meaning (e.g. default, default mode, DMN,
288 network DMN, default network), only the word with the highest correlation value was retained.
289 This analysis provides additional evidence about the functional role of the regions within

290 different maps, by comparing the results to previous studies which have reported similar
291 patterns of activation.

292 Finally, we wanted to examine whether the observed pattern of BOLD response in DMN
293 regions reflected the macroscale cortical organization captured by the principal gradient
294 (Margulies et al., 2016). In line with previous studies by our group (Murphy et al., 2018, 2019),
295 this analysis leverages the explanatory power of the unimodal to heteromodal gradient to
296 account for differences between experimental conditions. Consistently with our predictions of
297 greater DMN recruitment during information integration, we expected to observe a higher
298 response in regions towards the heteromodal end of the gradient in the 2>1 contrast. Decile
299 bins along the gradient were calculated using the methods outlined by Margulies et al. (2016).
300 The original gradient map provided values from 0 to 100 for each voxel in the brain (0 =
301 unimodal end; 100 = DMN). This map was then divided into ten-percentile bins: all voxels with
302 values 0–10 were assigned to bin1; voxels with values 11–20 to bin 2, etc., yielding 10 bins in
303 total. The total number of voxels in each bin was near-identical (each contained 6133 to 6135
304 voxels). This analysis provides unique insights by focusing on whole-brain patterns associated
305 with particular aspects of cued semantic retrieval, as opposed to the role of specific brain
306 regions. The analysis can establish whether peaks associated with cue integration across the
307 cortex are located at the apex of the gradient from heteromodal to unimodal processing, in
308 line with the expectation that heteromodal cortex supports information convergence.

309

310 3. RESULTS

311 3.1 Behavioural results

312 A repeated measures ANOVA examining response efficiency revealed no significant differences
313 across conditions [$F(3,75) = .62, p = .605, \eta^2 = .02$], indicating that semantic decisions following
314 two cues were not easier than trials with less contextual support (one cue or no cue). The
315 means and standard error for each condition are provided in Figure S1 and Table S1
316 (Supplementary Materials). There were also no significant differences between conditions in
317 accuracy [$F(3,75) = .14, p = .939, \eta^2 = .01$], median response time [$F(3,75) = .95, p = .420, \eta^2 =$
318 $.04$] or response time variability [$F(3,75) = 1.26, p = .296, \eta^2 = .05$]. All statistical values are
319 provided in Table S2.

320 *3.2 fMRI results*

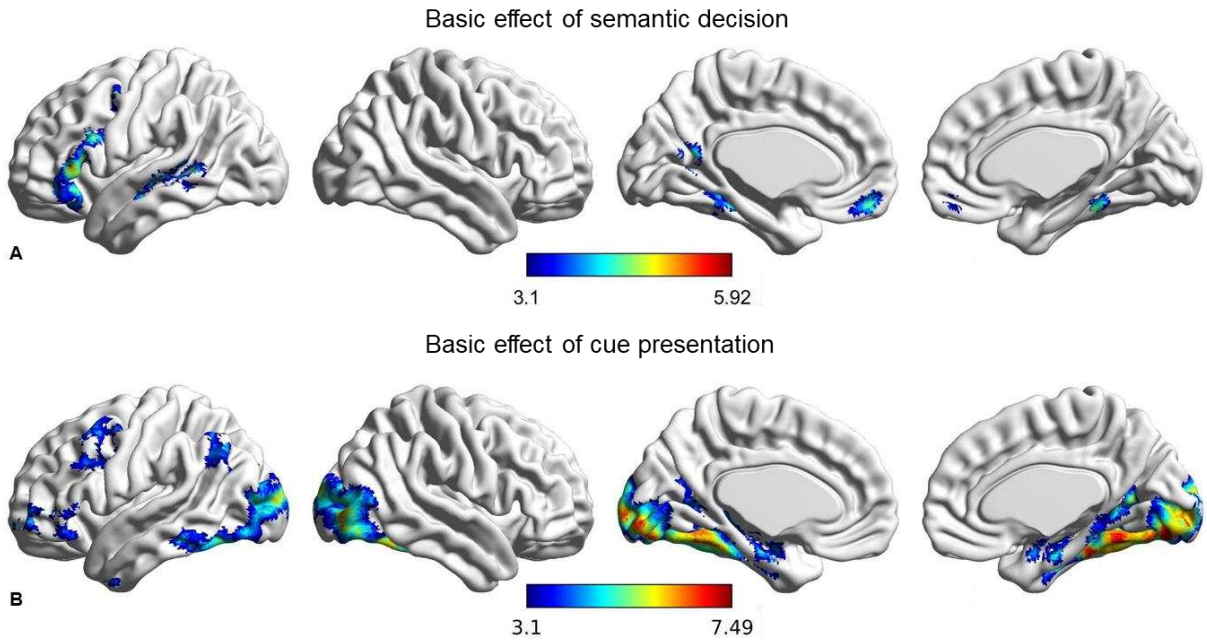
321 First, we report the whole-brain univariate results for models examining (i) how the BOLD
322 response during semantic decision-making changes as a consequence of cues (semantic
323 decision model) and (ii) the response to cue presentation (cue model). The coordinates for
324 cluster peaks are reported in Table S3 (Supplementary Materials) and statistical maps are
325 available in Neurovault (<https://neurovault.org/collections/6198/>). Next, to test one account of
326 the response to single cues vs. no cues during semantic decision-making, we present a region
327 of interest (ROI) analysis examining the response to different numbers of cues during cue
328 presentation, in regions defined by the semantic decision model. This exploratory analysis
329 establishes whether these regions behave in a load-dependent manner during cue encoding.
330 Finally, we examine whether integration effects in DMN regions are captured by a macroscale
331 gradient of cortical organization, using a series of ROIs positioned from the heteromodal to the
332 unimodal end of this gradient. Figures were created using BrainNet Viewer (Xia et al., 2013;
333 <http://www.nitrc.org/projects/bnv/>) and Surf Ice (<https://www.nitrc.org/projects/surfire/>).

334 3.2.1 Whole-brain results

335 *Semantic decision model*

336 Figure 2A shows the contrast between uncued semantic decisions and responses to letter
337 strings (also uncued), while Figure 3 shows the response to different cue contrasts (1 cue vs. 0
338 cues; 2 cues vs. 1 cue). The supplementary materials provide contrasts between semantic and
339 letter string trials for each of the cue conditions separately (Figure S3). These maps show a
340 similar semantic response across conditions, which resembles the contrast of 0 cues over letter
341 strings.

342 The contrast between semantic decisions without cues and non-semantic trials revealed
343 activation in brain areas previously associated with semantic cognition (in studies that largely
344 did not employ cues; e.g. Binder et al., 2009; Noonan et al., 2013; Seghier et al., 2004; Bright
345 et al., 2004; Gold et al., 2005; Chee et al., 2000; for reviews see Lambon Ralph et al., 2016;
346 Jefferies, 2013; Hoffman et al., 2018), in left-hemisphere semantic areas such as inferior frontal
347 gyrus and posterior temporal gyrus, as well as in medial temporal lobes, medial prefrontal and
348 posterior cingulate cortex (Figure 2A).



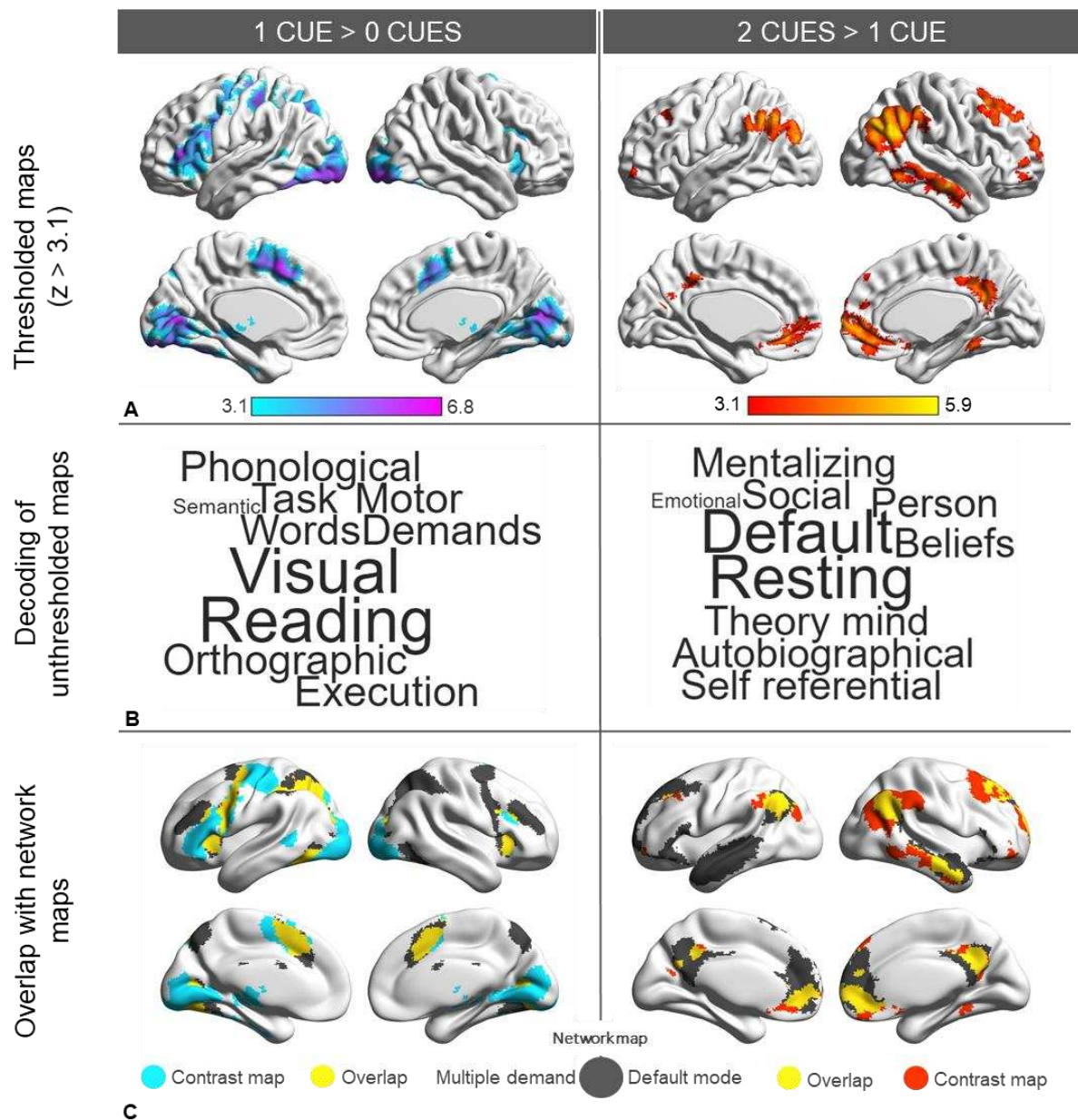
349

350 Figure 2. A. Basic effect of uncued semantic decision (semantic no cue > letter strings at decision time period). B.
 351 Basic effect of cue presentation (2 cues + 1 cue > 0 cue at cue time period). Coordinates of cluster peaks for these
 352 basic comparisons are reported in Table S3.

353 We then explored cueing effects by contrasting semantic decisions in the presence of different
 354 levels of constraint. The contrast of semantic decisions following 1 cue > 0 cues identified
 355 clusters in task-positive regions overlapping with the MDN (Duncan, 2010), consistent with the
 356 cognitive demands of maintaining cues. We found recruitment of inferior and middle frontal
 357 gyrus (with the peak in inferior frontal sulcus), precentral gyrus, bilateral paracingulate gyrus
 358 and pre-supplementary motor area, temporo-occipital cortex and visual cortex. Interestingly,
 359 the effect of multiple cues compared with a single cue (2>1) did not elicit stronger activation
 360 within these regions, even though the amount of information to be maintained was increased.
 361 Instead, this contrast elicited activation in regions overlapping with the DMN, including in
 362 bilateral angular gyrus/lateral occipital cortex, middle temporal gyrus, medial prefrontal
 363 cortex, posterior cingulate cortex, and left middle frontal gyrus. The thresholded maps for the
 364 two contrasts can be found in Figure 3 (top panel). Parameter estimates for the three
 365 conditions over the implicit baseline were extracted in both the 1>0 cue and 2>1 cue regions
 366 (see Supplementary Figure S4). Overall, 1>0 regions showed task-related activation (with more
 367 activation when cues had to be maintained in working memory, compared with the no cue
 368 condition) while 2>1 regions exhibited task-related deactivation (with less deactivation when
 369 people made semantic decisions following 2 convergent cues compared with 0 or 1 cue).

370 We examined the overlap of the contrast maps with published maps of the MDN (Duncan,
371 2010) and DMN (Yeo et al., 2011; Figure 3 - bottom). Consistent with the hypothesized role of
372 DMN in semantic integration, 36.2% of the total voxels in the 2>1 cue map overlapped with
373 the DMN, while only 1% of voxels overlapped with MDN. For the 1>0 cue map, the opposite
374 pattern was observed, with 31.8% of total voxels overlapping with MDN and only 2.4 % with
375 DMN. We submitted the unthresholded z maps for the 2>1 and 1>0 cue contrasts to
376 Neurosynth for cognitive decoding and produced word clouds using the top 10 terms positively
377 associated with the maps (Figure 3 – middle). The terms recovered for the 2>1 and 1>0 cue
378 maps suggest the involvement of DMN and MDN respectively. The contrast of 2 > 0 cues
379 (Figure S3), shows activation in regions overlapping with 1 > 0, such as left middle and inferior
380 frontal gyrus, left middle temporal gyrus, but also in regions within the 2 > 1 map, such as left
381 angular gyrus. This pattern of activation suggests that both cue maintenance and cue
382 integration might be visible in this map.

383 As the DMN is known to show anti-correlation with task-positive regions captured by the MDN
384 (Blank et al., 2014; Davey et al., 2016; Fox et al., 2005), we also explored whether this would
385 be the case for our contrast maps. In an independent sample of 86 participants, whole-brain
386 connectivity maps for the 2>1 and 1>0 contrasts were generated using CONN (Whitfield-
387 Gabrieli & Nieto-Castanon, 2012). Full methods are in the Supplementary Materials. The
388 analysis revealed two functionally distinct and anti-correlated networks, comprising DMN for
389 the 2>1 cue contrast and MDN regions involved in domain-general executive control for the
390 1>0 cue contrast (Figure S5).



391

392 Figure 3. Results for the main contrasts of interest in the semantic decision model: the left side of the figure
 393 contains results for 1 cue > 0 cues, while the 2 cues > 1 cue contrast is shown on the right. A. Contrast maps
 394 thresholded at $z > 3.1$. B. Word clouds produced by plotting the top 10 terms positively associated with the
 395 contrast map. C. Overlap of the 1 > 0 contrast with the multiple demand network (Duncan et al., 2010) and the
 396 contrast of 2 > 1 with the default mode network (Yeo et al., 2011).

397 *Cue model*

398 To check whether the two distinct networks identified as relevant for conceptual cueing also
 399 showed different responses to load during the encoding of cue information, we constructed a
 400 second model to look at the cue presentation period. This was an exploratory analysis, since
 401 our main focus was on how cues modulate the neural basis of semantic decisions. Our

402 paradigm was not designed to deconfound the order of the cues and the semantic decisions.
403 Nevertheless, if the regions showing a stronger response to semantic decisions following 1 vs.
404 0 cues reflect the working memory demands of cue maintenance, we would expect to see load-
405 dependent effects from cue encoding in these regions – i.e. stronger responses when more
406 cues are presented.

407 First, we used a contrast of 2 cues + 1 cue > 0 cues across the whole brain to define the basic
408 effect of cue presentation (see Figure 2B). This elicited bilateral activation in occipital visual
409 regions, extending into the posterior ventral stream in the left hemisphere. In addition, we
410 found bilateral recruitment of the inferior frontal sulcus (IFS), within the multiple demand
411 network, and the inferior frontal gyrus, in line with the idea of load demands of processing and
412 maintaining cues (this interpretation is further explored in paragraph 3.2.2 ‘ROI analysis of cue
413 load). Activation in the left hemisphere was also observed in AG.

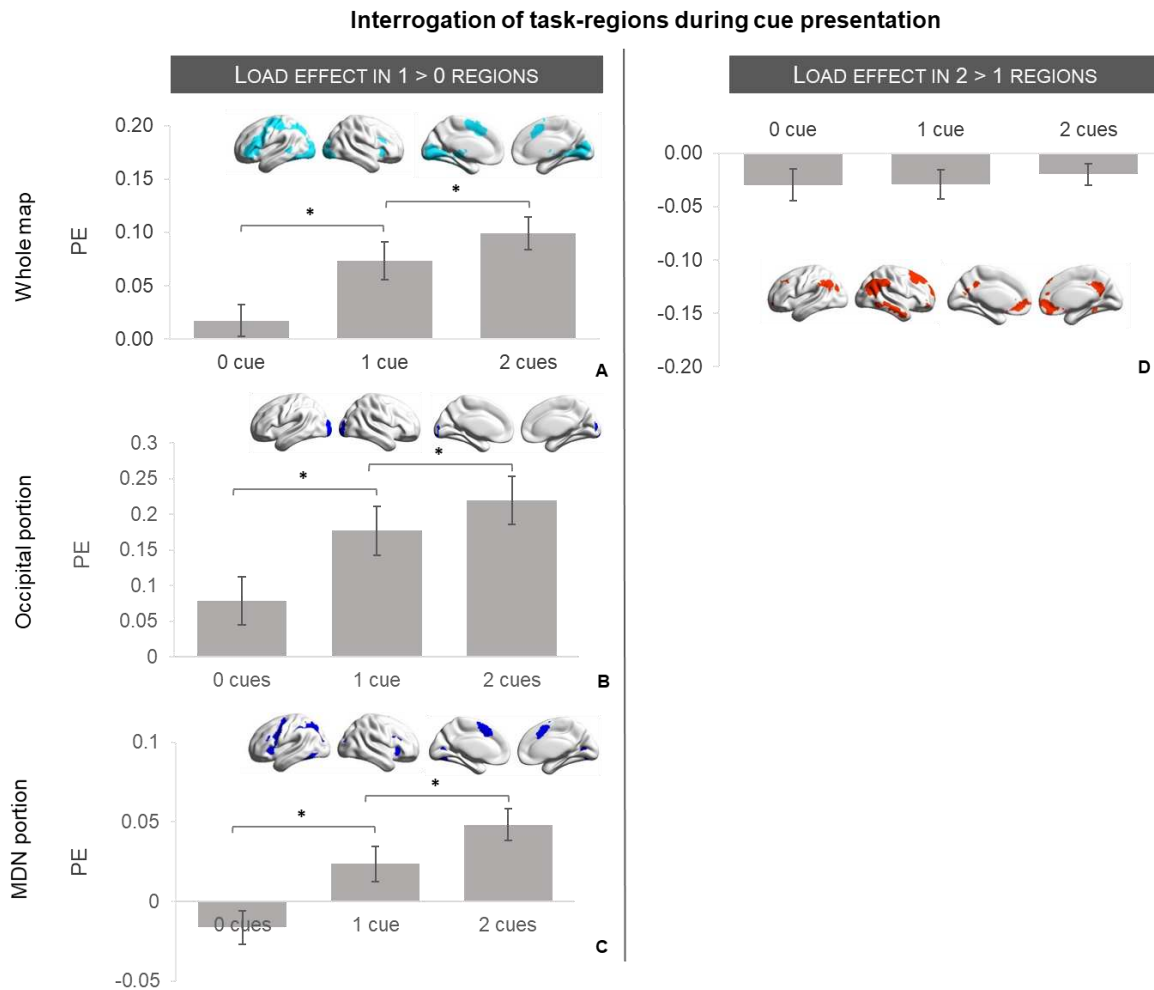
414 The Supplementary Figure S2 shows other cue presentation contrasts. The contrast of 2 > 0
415 cue presentation revealed activation in occipital cortex and in left-hemisphere control regions.
416 Similar control regions were recruited by the contrast of 2 > 1 cue presentation, although this
417 map had less extensive activation overall. The contrast of 1 cue > 0 cue presentation revealed
418 activity in visual regions largely overlapping with 2 cues > 0 cues, and a cluster in left angular
419 gyrus. Finally, the contrast of 1 cue location > 1 cue affect recruited visual regions in occipital
420 cortex and bilateral paracingulate gyrus, while the reverse contrast did not yield significant
421 results.

422 3.2.2 ROI analysis of cue load

423 To test possible accounts of the different patterns of activation observed in the decision-
424 making phase (*semantic decision model*) for the contrasts of 2 > 1 and 1 > 0 cues, we conducted
425 a post-hoc ROI analysis of the activation in these regions prior to the decision, when the cues
426 were on the screen (*cue model*). The recruitment of cognitive control areas (i.e. inferior and
427 middle frontal gyrus, inferior frontal sulcus, precentral gyrus, anterior cingulate gyrus, and pre-
428 supplementary motor area, falling within the multiple demand network) for semantic decisions
429 that followed the presence vs. absence of cues (1 > 0 cues) suggests that these regions might
430 be engaged in active maintenance of task-relevant information; in which case, cues might be
431 processed in a load-dependent way during the cue period. To test this idea, the regions that

432 responded to the contrasts of 1>0 and 2>1 cues during the semantic task (semantic decision
433 model) were used to mask the BOLD response for cue presentation (cue model). We extracted
434 and compared the parameter estimates for the three conditions against the implicit baseline:
435 no cues (scrambled images), one cue (average of face emotion and location cue) and two cues
436 (both face emotion and location image presented). If the semantic task activation observed for
437 the 1>0 contrast reflects a demand-relevant state associated with maintaining the cues, then
438 the activation of these regions during cue presentation should increase as the number of cues
439 is increased; i.e. 2 cues > 1 cue, 1 cue > 0 cues. This is because information about the cues is
440 required to be maintained from their onset. In contrast, regions responding more to semantic
441 decisions following multiple cues (2>1 cues) might not be expected to show a load-dependent
442 effect during the cue period. These regions responded more when multiple sources of
443 information could be used to constrain semantic retrieval – and this form of information
444 integration is unlikely to occur prior to the onset of the semantic decision (since the cues
445 themselves were not easy to link in the absence of the probe concept – for example HAPPY FACE
446 and SUPERMARKET are consistent with a wide range of concepts and do not strongly prime JAM).
447 Consistent with these predictions, we found that activation in the 1>0 cue regions increased in
448 a linear fashion with a higher number of cues [$F(1, 25) = 48.39, p < .001, \eta^2 = .66$] (Figure 4A).
449 However, there was no significant difference between cue conditions within regions
450 responsive to the 2>1 cue contrast [$F(2, 50) = .39, p = .682, \eta^2 = .02$] (Figure 4D).

451 The results of this ROI analysis show that regions responding more to semantic decisions
452 following 1 > 0 cues also respond in a load-dependent way during the encoding of cue
453 information. However, this ROI map includes both cognitive control regions within MDN and
454 visual cortex, making it difficult to separate the effects of increasing visual stimulation from
455 cognitive load. To further characterize the effect, we divided the 1 > 0 semantic decision map
456 into regions that fell within the occipital cortex (Harvard-Oxford probabilistic map – 25%) and
457 outside MDN regions (1997 voxels – Figure 4B), and within MDN after masking out occipital
458 regions (10658 voxels – Figure 4C). The BOLD response showed a similar linear increase with
459 the number of cues presented on the screen in visual cortex ($F(1, 25) = 54.96, p < .001, \eta^2 =$
460 $.69$) and in MDN ($F(1, 25) = 53.73, p < .001, \eta^2 = .68$).



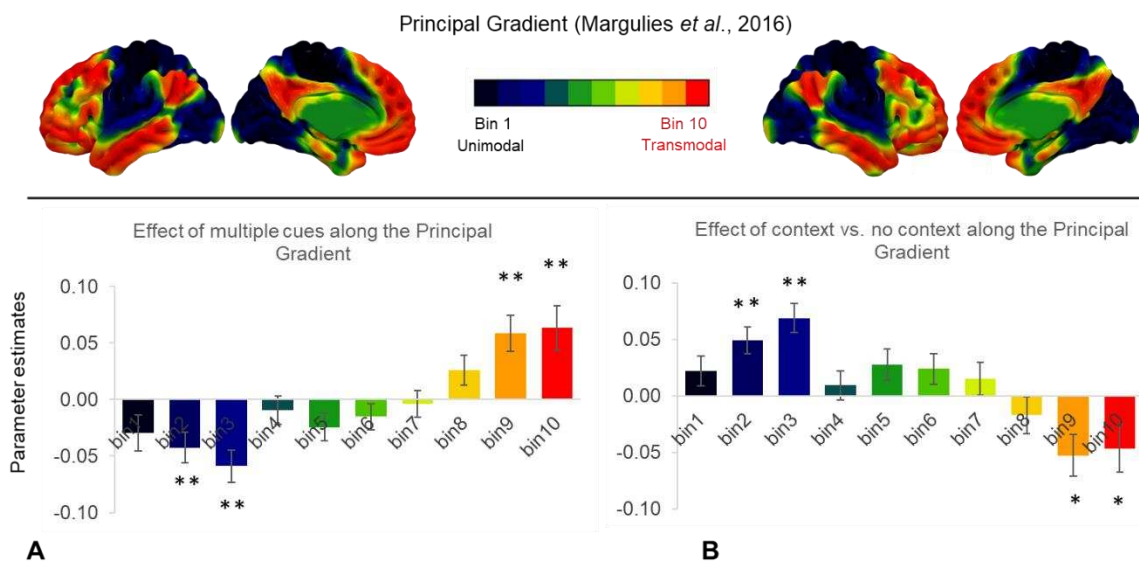
461

462 Fig 4. ROI analysis extracting the parameter estimates (PE) for the three levels of cue processing over the implicit
 463 baseline (cue model) in the 1 > 0 and 2 > 1 maps obtained in the semantic decision model. Three separate ROIs
 464 were conducted for the 1 > 0 regions (left panel): whole map (A), voxels that fell within the occipital cortex (B)
 465 and voxels that fell in the MDN (C). While the effect of number of cues is present in the 1 > 0 regions across the
 466 different masks used, no effect is observed in the integration regions (D) at the time-point of processing cue
 467 pictures. Bonferroni-corrected pairwise comparisons in the 1 > 0 regions confirmed that PE for 0 cues were
 468 significantly lower than 1 cue, and PE for 1 cue were significantly lower than 2 cues (all p values < .025; p value
 469 corrected for 2 multiple comparisons).

470 3.2.3 Gradient analysis

471 To further characterize the involvement of DMN regions in integrating information, we
 472 interrogated the response to semantic decisions along the Principal Gradient (Margulies et al.,
 473 2016). Unlike traditional univariate activation maps, which localize activation in certain regions,
 474 this gradient analysis examines how the effect of cueing unfolds along the entire cortical
 475 surface and measures the contribution of different portions of the gradient to the effects of

476 interest. This analysis can highlight systematic functional change along the cortical surface, and
 477 explain why similar functional transitions are observed in multiple locations. The gradient map
 478 was divided into 10-percentile bins (see Methods section) and each bin was used as a mask in
 479 ROI analyses where we extracted mean parameter estimates for the contrasts of 2 cues vs. 1
 480 cue and 1 cue vs. 0 cues within each bin (see Figure 5). We then explored the effect of gradient
 481 bin on each univariate contrast using a two-way repeated measure ANOVA with *cue contrast*
 482 (2 levels: 2 cues vs.1 cue and 1 cue vs. 0 cues) and *gradient bin* (10 levels) as within-subject
 483 variables. This analysis revealed a significant interaction of cue contrast and gradient bin ($F(2,$
 484 $51) = 28.33, p < .001, \eta^2 = .53$), suggesting that the effect of gradient was different for $2 > 1$ and
 485 $1 > 0$ contrasts. Next, we performed two one-way repeated measure ANOVAs looking at the
 486 effect of *gradient bin* on each contrast separately. For $2 > 1$ cues, we found a significant linear
 487 effect for gradient bin ($F(1, 25) = 47.13, p < .001, \eta^2 = .65$), as well as complex higher-order
 488 contrast effects (values reported in Table S5). The comparison of semantic decisions following
 489 2 vs. 1 cues elicited maximal activity at the heteromodal end of the gradient, suggesting that
 490 DMN regions at this end of the principal gradient responded more strongly when multiple
 491 sources of information were integrated to support semantic cognition. For $1 > 0$ cues, we found
 492 the opposite pattern, with more activation at the unimodal end of the gradient for the single
 493 cue condition compared to when no cues were provided. Again, the effect of context vs. no-
 494 context along the principal gradient was complex, with linear ($F(1, 25) = 24.80, p < .001, \eta^2 =$
 495 $.50$), as well as higher-order contrasts reaching significance. Full details of the statistical
 496 outcomes are reported in Supplementary Tables S4, S5, S6.



497

498 Figure 5. A. Semantic decisions in the presence of multiple cues (contrast of 2>1 cues) maximally recruited regions
499 at the heteromodal end of the principal gradient. B. The effect of context vs. no context (contrast of 1>0 cues)
500 showed an effect in the opposite direction, with maximal activation toward the sensory end of the gradient. **
501 Highlights portions of the gradient where the BOLD response is significantly different from 0 when the Bonferroni
502 correction is applied (all p values $\leq .005$), while * denotes p values $< .05$.

503

504 4 DISCUSSION

505 Recent accounts of the default mode network (DMN) place this system at the top of a
506 cortical hierarchy, maximally distant from unimodal sensory regions (Margulies et al., 2016) in
507 both geodesic and connectivity space. The separation of heteromodal DMN regions from
508 unimodal cortex may underpin our capacity to form conceptual representations that are not
509 dominated by a particular type of feature but instead draw on multiple types of information –
510 including affect or spatial location. To test this idea, we contrasted semantic decisions made
511 following the presentation of multiple cues (depicting facial emotional expressions and
512 locations), only one of these cues, or no cues. In this way, we manipulated the extent to which
513 semantic retrieval occurred in a rich and meaningful context, in which multiple convergent
514 features were available. Our results indicate that the cueing paradigm involved distinct mental
515 processes that were supported by different networks. First, from the onset of the cues,
516 information was maintained in working memory: MDN regions were activated for the contrast
517 1 cue > 0 cues, and the response of these regions during cue presentation was load-dependent.
518 These findings are in line with previous research showing that the multiple demand network
519 supports the maintenance of goal-relevant information (Duncan, 2010; Woolgar et al., 2011).
520 Secondly, DMN regions were activated by the contrast 2 cues > 1 cue, consistent with a role of
521 this network in convergent information integration. In line with our prediction that information
522 integration occurs at the heteromodal end of the Principal Gradient, we found greater
523 recruitment at this end when semantic decisions occurred in the presence of multiple cues. In
524 contrast, activation was greater towards the unimodal end of the gradient (in regions
525 overlapping with visual cortex) when semantic decisions were made in the presence vs.
526 absence of cues. These novel findings provide important insights into the neural mechanisms
527 supporting semantic integration and suggest a framework for understanding the location of
528 these effects at the heteromodal end of the principal gradient.

529 According to “task-negative” accounts of the DMN, apparent semantic activation of this
530 network occurs when an easy task is contrasted with a hard task (Humphreys et al., 2015;
531 Humphreys et al., 2019; Humphreys & Lambon Ralph, 2014). This account is unlikely to provide
532 an adequate explanation of our data since we found no behavioural differences between
533 conditions (unlike other reports of cueing effects; Lanzoni et al., 2019; Noonan et al., 2010;
534 Rodd et al., 2016, 2013). Our findings are instead consistent with a rich neuroimaging literature
535 implicating ATL and AG in the formation of conceptual combinations. Integrating items (e.g.
536 “jacket” and “plaid”) into coherent concepts (i.e. “plaid jacket”) modulates activity in AG
537 regardless of the modality of presentation, while atrophy in this region results in impaired
538 conceptual combinations (Price et al., 2015; see also Price et al., 2016). Similarly,
539 magnetoencephalography (MEG) studies show increased activity in left ATL and AG for
540 meaningful conceptual combinations (e.g. “red boat”) compared to the same words preceded
541 by unpronounceable consonant strings (e.g. “xkq boat; Bemis & Pylkkänen, 2011; 2013;
542 Pylkkänen, 2019), particularly when these combinations are more predictable or share more
543 overlapping semantic features (Teige et al., 2019). Activation in the left superior ATL is also
544 observed during semantic decisions following meaningful sentence cues, while IFG shows the
545 opposite pattern (i.e. increased activation following irrelevant vs. relevant contexts), consistent
546 with a role in semantic control (Hoffman et al., 2015). Moving beyond the language stimuli
547 used in previous studies on conceptual combinations, here we show that semantic integration
548 in DMN occurs for non-verbal material (i.e. pictures), in line with the heteromodal nature of
549 these regions. Our findings uniquely add to this literature by showing that these effects of
550 conceptual combination are maximal at the heteromodal end of the principal gradient, which
551 situates DMN at the top of functional hierarchy (Margulies et al., 2016). Consequently, effects
552 of information integration are seen not only in classic semantic regions such as AG and anterior
553 middle temporal gyrus, but also in other DMN regions highlighted by our 2 > 1 cues contrast
554 (e.g., superior frontal gyrus; medial prefrontal and posterior cingulate cortex).

555 The role of DMN in semantic cognition appeared to be largely restricted to the impact
556 of convergent cueing during semantic decision-making: in contrast, a distinct anti-correlated
557 network overlapping with MDN was associated with the selective attention and working
558 memory demands of encoding and maintaining individual cues. Moreover, the basic effect of
559 making semantic decisions in the absence of cues, relative to the letter string trials, did not

560 reveal activation in DMN regions. At first, this result may seem at odds with accounts of the
561 DMN that attribute a crucial role in semantic cognition to this network. However, our semantic
562 task was considerably more demanding than the letter string baseline: studies have shown that
563 although DMN regions can respond to the contrast of semantic vs. non-semantic tasks, they
564 typically do so when the semantic task is not more demanding than the comparison task
565 (Binder et al., 2009; Humphreys et al., 2015). Moreover, activation in DMN regions is often
566 associated with ‘automatic’ patterns of retrieval or conceptual combinations (Davey et al.,
567 2016; Teige et al., 2019; Price et al., 2016, Bemis & Pykkänen, 2011; 2013), while our task
568 required participants to match an ambiguous words to a target word while discarding
569 distractors and as such, it might involve more ‘controlled’ aspects of retrieval supported by
570 regions such as left IFG which lie outside DMN.

571 In line with other studies, we found that DMN regions responding to cue integration
572 (i.e. the 2>1 cue contrast during semantic decisions) showed differential deactivation across
573 conditions, relative to the implicit baseline, while MDN regions responding to cue maintenance
574 (i.e., the 1>0 cue contrast during semantic decisions) showed differential activation. The
575 functional significance of task-related deactivation is a topic of considerable debate; while
576 some authors have interpreted deactivation as suggesting that sites are irrelevant to ongoing
577 cognition (e.g. Humphreys et al., 2015), another possibility is that deactivation might be
578 functionally relevant, as it might allow DMN regions to integrate information more selectively
579 from task-relevant networks (Krieger-Redwood et al., 2016). According to this “cognitive
580 tuning” hypothesis, we might expect more deactivation of DMN regions when only a limited
581 set of features are relevant to ongoing cognition (for example, in the 0 and 1 cue conditions,
582 when emotion and location representations are not necessarily task-relevant). There are
583 already studies demonstrating that DMN regions can increase their coupling to cognitive
584 control areas when harder tasks are contrasted with easier tasks, even as they deactivate
585 (Krieger-Redwood et al., 2016; Vatansever et al., 2015; 2017).

586 The effect of convergent cueing was not found within one specific semantic region,
587 such as AG, but across multiple distributed nodes of DMN. We then turned to the Principal
588 Gradient of intrinsic connectivity to provide a potential explanation for why cue integration
589 effects were observed where they were across the cortex. The separation between DMN and
590 unimodal systems, captured by the Principal Gradient, is thought to (i) allow heteromodal

591 representations to emerge (cf. Hub and Spoke account) and (ii) support forms of cognition that
592 require separation from the external environment, such as states that draw on heteromodal
593 representations in memory. The latter observation is particularly important for explaining the
594 similarity of our results with recent findings from our group (Murphy et al., 2018, 2019). Using
595 a 1-back/0-back paradigm, Murphy et al. showed that decisions based on the immediately
596 available perceptual input (0 back condition) elicited higher activity towards the unimodal end
597 of the Principal Gradient, while decisions drawing on information from memory (1 back
598 condition) maximally recruited the heteromodal end of the gradient (Murphy et al., 2019).
599 Critically, DMN involvement in memory-guided cognition was maximised when the decisions
600 involved meaningful objects that were not perceptually-identical, increasing reliance on
601 conceptual knowledge, relative to simpler unidimensional decisions based on colour (Murphy
602 et al., 2018). Building on these findings, the results of the current study suggest that this
603 pattern of activation within DMN arises because heteromodal cortex at the top end of the
604 gradient supports the integration of disparate and convergent sources of information; these
605 regions are more involved when we match meaningful objects based on their identities
606 extracted from a multitude of features, as opposed to single features. Nevertheless, Murphy
607 et al. also showed that tasks based on memory recruit representations at the heteromodal end
608 of the gradient, even when these tasks only probe a single feature and therefore arguably do
609 not place strong demands on information integration: this pattern might arise because in the
610 absence of perceptual inputs, heteromodal regions may play a key role in generating patterns
611 of cognition needed for the task (i.e., visual imagery). Importantly, the regions at the top of the
612 gradient responded similarly to memory-based decisions irrespective of whether these
613 decisions concerned colour or shape; in this way, the function of these sites still reflects the
614 heteromodal nature of DMN. In contrast, distinct unimodal sites responsive to colour and
615 shape are expected to support these decisions when perceptual information is present. In
616 summary, the principal gradient relating to the separation of heteromodal from unimodal
617 processing can potentially explain both the increased response in heteromodal DMN when
618 cognition involves multiple convergent features, and the common response in heteromodal
619 DMN when cognition involves decisions about single features in the absence of perceptual
620 input.

621 There are a number of limitations of this study. It does not fully establish the form of
622 the relationship between the number of cues and DMN activation at retrieval, since we did not
623 manipulate cueing parametrically. Activation in DMN regions may not increase linearly with
624 the number of cues (0, 1, 2 cues). Instead, the contrast of 1 > 0 cues elicits activation in MDN
625 regions and towards the unimodal end of the principal gradient, suggesting that the presence
626 vs. absence of context involves additional cue encoding and maintenance in working memory.
627 A follow up study could use a parametric manipulation of the number of cues to better identify
628 how responses in MDN and DMN scale with the number of cues. Moreover, in our experiment,
629 integration unfolded over time, with semantic decisions occurring roughly 2 seconds after the
630 presentation of the cue. A recent study by Branzi and others (2019) suggests that ventral AG
631 supports the integration of meanings during time-extended narratives (see also Bonnici et al.,
632 2016; Ramanan et al., 2017). Future research should establish whether semantic integration
633 that emerges over time leads to a different pattern of activation along the principal gradient
634 compared with the integration of simultaneously-presented information.

635 Furthermore, although our cueing paradigm allowed us to recover a set of regions
636 within DMN recruited during semantic integration, it is unclear whether we would observe the
637 same pattern of activation with other types of cues. Future studies could examine tasks that
638 involve simple sensory features, for example, semantic decisions about concrete concepts such
639 as DOG following visual and auditory feature cues (e.g. image of tail and sound of dog barking)
640 to establish if a similar integration effect occurs in DMN. The current experiment used complex
641 stimuli depicting emotional affect and locations, which are known to be relevant to the DMN.
642 The DMN is closely associated with the classic limbic network for emotional processing (e.g.
643 Chanes & Barrett, 2016; Greicius et al., 2003; Raichle et al., 2001; Simpson et al., 2000).
644 Moreover, the hippocampus, which has strong functional ties with the default mode network
645 (Andrews-Hanna et al., 2010; Kernbach et al., 2018 ; Leech & Sharp, 2014; Raichle et al., 2001)
646 is known to play a role in representing spatial locations (e.g. Bellmund et al., 2016; Burgess,
647 2002; Burgess et al., 2002; Robin et al., 2018). Our findings demonstrate that when semantic
648 decisions are made in the context of both emotional and spatial information, as opposed to
649 only one of these cue types, DMN ramps up its response in line with its hypothesised role in
650 higher-order information integration. Contrary to previous literature showing the recruitment
651 of the parahippocampal place area for spatial scenes (e.g. Epstein & Kanwisher, 1998) and the

652 fusiform face area for faces (e.g. Kanwisher et al., 1997), our contrasts of 1 cue type over the
653 other aligned only partially with previous evidence. The failure to reach statistical significance
654 for the contrast of 1 cue affect > 1 cue location could reflect a lack of statistical power, since
655 much of the data acquisition was devoted to the semantic decisions. Moreover, the different
656 size and aspect ratio of the images (with location images being wider and larger) may have
657 influenced the results.

658 A final limitation of the study concerns the statistical model used to examine activation
659 during cue presentation, which was used to test possible interpretations of the univariate
660 results in the main model in a post-hoc fashion. As the experiment was not originally designed
661 to look at the cue presentation, we did not include trials in which facial expressions and
662 location cues were not followed by semantic decisions. Whenever a meaningful cue picture
663 was presented, this was always followed by a semantic decision. The inclusion of trials where
664 cues were followed by a blank screen would have facilitated the temporal separation of the
665 cue and task events, allowing us to draw stronger conclusions from the cue model. In this way,
666 future research could directly test the idea that integration requires a component of
667 maintenance supported by the MDN, in addition to a combination of conceptual features
668 within DMN.

669

670

671 **BIBLIOGRAPHY**

- 672 Andrews-Hanna, J. R., Reidler, J. S., Sepulcre, J., Poulin, R., & Buckner, R. L. (2010). Functional-
673 Anatomic Fractionation of the Brain's Default Network. *Neuron*, *65*(4), 550–562.
674 <https://doi.org/10.1016/j.neuron.2010.02.005>
- 675 Badre, D., & Wagner, A. D. (2005). Frontal lobe mechanisms that resolve proactive
676 interference. *Cerebral Cortex*, *15*(12), 2003–2012.
677 <https://doi.org/10.1093/cercor/bhi075>
- 678 Badre, D., & Wagner, A. D. (2006). Computational and neurobiological mechanisms
679 underlying cognitive flexibility. *Proceedings of the National Academy of Sciences of the*
680 *United States of America*, *103*(18), 7186–7191.
681 <https://doi.org/10.1073/pnas.0509550103>
- 682 Beckmann, C. F., Jenkinson, M., & Smith, S. M. (2003). General multilevel linear modeling for
683 group analysis in FMRI. *NeuroImage*, *20*(2), 1052–1063. [https://doi.org/10.1016/S1053-](https://doi.org/10.1016/S1053-8119(03)00435-X)
684 [8119\(03\)00435-X](https://doi.org/10.1016/S1053-8119(03)00435-X)
- 685 Behzadi, Y., Restom, K., Liu, J., & Liu, T. T. (2007). A component based noise correction
686 method (CompCor) for BOLD and perfusion based fMRI. *NeuroImage*, *37*(1), 90–101.
687 <https://doi.org/10.1016/j.neuroimage.2007.04.042>
- 688 Bellmund, J. L. S., Deuker, L., Schröder, T. N., & Doeller, C. F. (2016). Grid-cell representations
689 in mental simulation. *eLife*, *5*(AUGUST), 1–21. <https://doi.org/10.7554/eLife.17089>
- 690 Bemis, D. K., & Pylkkänen, L. (2011). Simple Composition: A Magnetoencephalography
691 Investigation into the Comprehension of Minimal Linguistic Phrases. *Journal of*
692 *Neuroscience*, *31*(8), 2801–2814. <https://doi.org/10.1523/JNEUROSCI.5003-10.2011>
- 693 Bemis, D. K., & Pylkkänen, L. (2013). Basic linguistic composition recruits the left anterior
694 temporal lobe and left angular gyrus during both listening and reading. *Cerebral Cortex*,
695 *23*(8), 1859–1873. <https://doi.org/10.1093/cercor/bhs170>
- 696 Binder, J. R., Desai, R. H., Graves, W. W., & Conant, L. L. (2009). Where Is the Semantic
697 System? A Critical Review and Meta-Analysis of 120 Functional Neuroimaging Studies.
698 *Cerebral Cortex*, *19*(12), 2767–2796. <https://doi.org/10.1093/cercor/bhp055>

- 699 Blank, I., Kanwisher, N., & Fedorenko, E. (2014). A functional dissociation between language
700 and multiple-demand systems revealed in patterns of BOLD signal fluctuations. *Journal*
701 *of Neurophysiology*, 112(5), 1105–1118. <https://doi.org/10.1152/jn.00884.2013>
- 702 Bonnici, H. M., Richter, F. R., Yazar, Y., & Simons, J. S. (2016). Multimodal Feature Integration
703 in the Angular Gyrus during Episodic and Semantic Retrieval. *Journal of Neuroscience*,
704 36(20), 5462–5471. <https://doi.org/10.1523/JNEUROSCI.4310-15.2016>
- 705 Branzi, F. M., Humphreys, G. F., Hoffman, P., & Ralph, M. A. L. (2019). Revealing the neural
706 networks that extract conceptual gestalts from continuously evolving or changing
707 semantic contexts. *BioRxiv*, 666370. <https://doi.org/10.1101/666370>
- 708 Bright, P., Moss, H., & Tyler, L. K. (2004). Unitary vs multiple semantics: PET studies of word
709 and picture processing. *Brain and language*, 89(3), 417-432.
710 <https://doi.org/10.1016/j.bandl.2004.01.010>
- 711 Brysbaert, M., Warriner, A. B., & Kuperman, V. (2014). Concreteness ratings for 40 thousand
712 generally known English word lemmas. *Behavior research methods*, 46(3), 904-911.
713 <https://doi.org/10.3758/s13428-013-0403-5>
- 714 Buckner, R. L., & Krienen, F. M. (2013). The evolution of distributed association networks in
715 the human brain. *Trends in Cognitive Sciences*, 17(12), 648–665.
716 <https://doi.org/10.1016/j.tics.2013.09.017>
- 717 Burgess, N. (2002). The hippocampus, space, and viewpoints in episodic memory. *The*
718 *Quarterly Journal of Experimental Psychology Section A*, 55(4), 1057–1080.
719 <https://doi.org/10.1080/02724980244000224>
- 720 Burgess, N., Maguire, E. A., & O'keefe, J. (2002). Review The Human Hippocampus and Spatial
721 and Episodic Memory appears to remain in humans (Abrahams et al. *Neuron*, 35, 625–
722 641. [https://doi.org/10.1016/S0896-6273\(02\)00830-9](https://doi.org/10.1016/S0896-6273(02)00830-9)
- 723 Chai, X. J., Castañán, A. N., Öngür, D., & Whitfield-Gabrieli, S. (2012). Anticorrelations in
724 resting state networks without global signal regression. *NeuroImage*, 59(2), 1420–1428.
725 <https://doi.org/10.1016/j.neuroimage.2011.08.048>
- 726 Chanes, L., & Barrett, L. F. (2016). Redefining the Role of Limbic Areas in Cortical Processing.

727 *Trends in Cognitive Sciences*, 20(2), 96–106. <https://doi.org/10.1016/j.tics.2015.11.005>

728 Chee, M. W., Weekes, B., Lee, K. M., Soon, C. S., Schreiber, A., Hoon, J. J., & Chee, M. (2000).
729 Overlap and dissociation of semantic processing of Chinese characters, English words,
730 and pictures: evidence from fMRI. *Neuroimage*, 12(4), 392-403.
731 <https://doi.org/10.1006/nimg.2000.0631>

732 Chiou, R., & Lambon Ralph, M. A. (2019). Unveiling the dynamic interplay between the hub-
733 and spoke-components of the brain's semantic system and its impact on human
734 behaviour. *NeuroImage*, 199(April), 114–126.
735 <https://doi.org/10.1016/j.neuroimage.2019.05.059>

736 Davey, J., Cornelissen, P. L., Thompson, H. E., Sonkusare, S., Hallam, G., Smallwood, J., &
737 Jefferies, E. (2015). Automatic and Controlled Semantic Retrieval: TMS Reveals Distinct
738 Contributions of Posterior Middle Temporal Gyrus and Angular Gyrus. *The Journal of*
739 *Neuroscience : The Official Journal of the Society for Neuroscience*, 35(46), 15230–
740 15239. <https://doi.org/10.1523/JNEUROSCI.4705-14.2015>

741 Davey, J., Thompson, H. E., Hallam, G., Karapanagiotidis, T., Murphy, C., De Caso, I., ...
742 Jefferies, E. (2016). Exploring the role of the posterior middle temporal gyrus in
743 semantic cognition: Integration of anterior temporal lobe with executive processes.
744 *NeuroImage*, 137, 165–177. <https://doi.org/10.1016/j.neuroimage.2016.05.051>

745 Dosenbach, N. U., Visscher, K. M., Palmer, E. D., Miezin, F. M., Wenger, K. K., Kang, H. C., ... &
746 Petersen, S. E. (2006). A core system for the implementation of task sets. *Neuron*, 50(5),
747 799-812. <https://doi.org/10.1016/j.neuron.2006.04.031>

748 Dumontheil, I., Thompson, R., & Duncan, J. (2011). Assembly and use of new task rules in
749 fronto-parietal cortex. *Journal of Cognitive Neuroscience*, 23(1), 168-182.
750 <https://doi.org/10.1162/jocn.2010.21439>

751 Duncan, J. (2010). The multiple-demand (MD) system of the primate brain: mental programs
752 for intelligent behaviour. *Trends in Cognitive Sciences*, 14(4), 172–179.
753 <https://doi.org/10.1016/j.tics.2010.01.004>

754 Epstein, R., & Kanwisher, N. (1998). A cortical representation of the local visual environment.
755 *Nature*, 392(6676), 598-601. <https://doi.org/10.1038/33402>

756 Fox, M. D., Snyder, A. Z., Vincent, J. L., Corbetta, M., Van Essen, D. C., & Raichle, M. E. (2005).
757 The human brain is intrinsically organized into dynamic, anticorrelated functional
758 networks. *Proceedings of the National Academy of Sciences of the United States of*
759 *America*, *102*(27), 9673–9678. <https://doi.org/10.1073/pnas.0504136102>

760 Gawlick-Grendell, L. A., & Woltz, D. J. (1994). Meaning dominance norms for 120
761 homographs. *Behavior Research Methods, Instruments, & Computers*, *26*(1), 5–25.
762 <https://doi.org/10.3758/BF03204557>

763 Gold, B. T., Balota, D. A., Kirchoff, B. A., & Buckner, R. L. (2005). Common and dissociable
764 activation patterns associated with controlled semantic and phonological processing:
765 evidence from fMRI adaptation. *Cerebral Cortex*, *15*(9), 1438-1450.
766 <https://doi.org/10.1093/cercor/bhi024>

767 Greicius, M. D., Krasnow, B., Reiss, A. L., & Menon, V. (2003). Functional connectivity in the
768 resting brain: A network analysis of the default mode hypothesis. *Proceedings of the*
769 *National Academy of Sciences of the United States of America*, *100*(1), 253–258.
770 <https://doi.org/10.1073/pnas.0135058100>

771 Hallam, G. P., Whitney, C., Hymers, M., Gouws, A. D., & Jefferies, E. (2016). Charting the
772 effects of TMS with fMRI: Modulation of cortical recruitment within the distributed
773 network supporting semantic control. *Neuropsychologia*, *93*(September), 40–52.
774 <https://doi.org/10.1016/j.neuropsychologia.2016.09.012>

775 Hoffman, P., Binney, R. J., & Ralph, M. A. L. (2015). Differing contributions of inferior
776 prefrontal and anterior temporal cortex to concrete and abstract conceptual
777 knowledge. *Cortex*, *63*, 250-266. <https://doi.org/10.1016/j.cortex.2014.09.001>

778 Hoffman, P., McClelland, J. L., & Lambon Ralph, M. A. (2018). Concepts, control, and context:
779 A connectionist account of normal and disordered semantic cognition. *Psychological*
780 *Review*, *125*(3), 293–328. <https://doi.org/10.1037/rev0000094>

781 Humphreys, G. F., Hoffman, P., Visser, M., Binney, R. J., & Lambon Ralph, M. A. (2015).
782 Establishing task- and modality-dependent dissociations between the semantic and
783 default mode networks. *Proceedings of the National Academy of Sciences*, *112*(25),
784 7857–7862. <https://doi.org/10.1073/pnas.1422760112>

785 Humphreys, G. F., Jackson, R. L., & Ralph, M. A. L. (2019). Overarching principles and
786 dimensions of the functional organisation in the inferior parietal cortex. *BioRxiv*, 44(0).
787 <https://doi.org/10.1101/654178>

788 Humphreys, G. F., & Lambon Ralph, M. A. (2014). Fusion and fission of cognitive functions in
789 the human parietal cortex. *Cerebral Cortex*, 25(10), 3547–3560.
790 <https://doi.org/10.1093/cercor/bhu198>

791 Jackson, R. L., Hoffman, P., Pobric, G., & Lambon Ralph, M. A. (2016). The Semantic Network
792 at Work and Rest: Differential Connectivity of Anterior Temporal Lobe Subregions. *The*
793 *Journal of Neuroscience : The Official Journal of the Society for Neuroscience*, 36(5),
794 1490–1501. <https://doi.org/10.1523/JNEUROSCI.2999-15.2016>

795 Jefferies, E. (2013). The neural basis of semantic cognition: Converging evidence from
796 neuropsychology, neuroimaging and TMS. *Cortex*, 49(3), 611–625.
797 <https://doi.org/10.1016/j.cortex.2012.10.008>

798 Jenkinson, M., Bannister, P., Brady, M., & Smith, S. (2002). Improved Optimization for the
799 Robust and Accurate Linear Registration and Motion Correction of Brain Images.
800 *NeuroImage*, 17(2), 825–841. <https://doi.org/10.1006/nimg.2002.1132>

801 Jenkinson, M., & Smith, S. (2001). A global optimisation method for robust affine registration
802 of brain images. *Medical Image Analysis*, 5(2), 143–156. [https://doi.org/10.1016/S1361-](https://doi.org/10.1016/S1361-8415(01)00036-6)
803 [8415\(01\)00036-6](https://doi.org/10.1016/S1361-8415(01)00036-6)

804 Kanwisher, N., McDermott, J., & Chun, M. M. (1997). The fusiform face area: a module in
805 human extrastriate cortex specialized for face perception. *Journal of neuroscience*,
806 17(11), 4302-4311. <https://doi.org/10.1523/JNEUROSCI.17-11-04302.1997>

807 Kernbach, J. M., Gramfort, A., Thirion, B., Thiebaut de Schotten, M., Sabuncu, M. R., Yeo, B. T.
808 T., ... Margulies, D. S. (2018). Subspecialization within default mode nodes characterized
809 in 10,000 UK Biobank participants. *Proceedings of the National Academy of Sciences*,
810 115(48), 12295–12300. <https://doi.org/10.1073/pnas.1804876115>

811 Krieger-Redwood, K., Teige, C., Davey, J., Hymers, M., & Jefferies, E. (2015). Conceptual
812 control across modalities: Graded specialisation for pictures and words in inferior frontal
813 and posterior temporal cortex. *Neuropsychologia*, 76, 92–107.

814 <https://doi.org/10.1016/j.neuropsychologia.2015.02.030>

815 Krieger-Redwood, K., Jefferies, E., Karapanagiotidis, T., Seymour, R., Nunes, A., Ang, J. W. A.,
816 ... & Smallwood, J. (2016). Down but not out in posterior cingulate cortex: Deactivation
817 yet functional coupling with prefrontal cortex during demanding semantic
818 cognition. *Neuroimage*, *141*, 366-377.
819 <https://doi.org/10.1016/j.neuroimage.2016.07.060>

820 Lambon Ralph, M. A., Jefferies, E., Patterson, K., & Rogers, T. T. (2016). The neural and
821 computational bases of semantic cognition. *Nature Reviews Neuroscience*.
822 <https://doi.org/10.1038/nrn.2016.150>

823 Langner, O., Dotsch, R., Bijlstra, G., Wigboldus, D. H. J., Hawk, S. T., & van Knippenberg, A.
824 (2010). Presentation and validation of the Radboud Faces Database. *Cognition and*
825 *Emotion*, *24*(8), 1377–1388. <https://doi.org/10.1080/02699930903485076>

826 Lanzoni, L., Thompson, H., Beintari, D., Berwick, K., Demnitz-King, H., Raspin, H., ... Jefferies, E.
827 (2019). Emotion and location cues bias conceptual retrieval in people with deficient
828 semantic control. *Neuropsychologia*, *131*(June), 294–305.
829 <https://doi.org/10.1016/j.neuropsychologia.2019.05.030>

830 Leech, R., & Sharp, D. J. (2014). The role of the posterior cingulate cortex in cognition and
831 disease. *Brain*, *137*(1), 12–32. <https://doi.org/10.1093/brain/awt162>

832 Margulies, D. S., Ghosh, S. S., Goulas, A., Falkiewicz, M., Huntenburg, J. M., Langs, G., ...
833 Smallwood, J. (2016). Situating the default-mode network along a principal gradient of
834 macroscale cortical organization. *Proceedings of the National Academy of Sciences of the*
835 *United States of America*, *113*(44), 12574–12579.
836 <https://doi.org/10.1073/pnas.1608282113>

837 Mesulam, M. M. (1998). From sensation to cognition. *Brain*, *121*(6), 1013–1052.
838 <https://doi.org/10.1093/brain/121.6.1013>

839 Mollo, G., Cornelissen, P. L., Millman, R. E., Ellis, A. W., & Jefferies, E. (2017). Oscillatory
840 dynamics supporting semantic cognition: Meg evidence for the contribution of the
841 anterior temporal lobe hub and modality-specific spokes. *PLoS ONE*, *12*(1), 1–25.
842 <https://doi.org/10.1371/journal.pone.0169269>

843 Murphy, C., Jefferies, E., Rueschemeyer, S. A., Sormaz, M., Wang, H. ting, Margulies, D. S., &
844 Smallwood, J. (2018). Distant from input: Evidence of regions within the default mode
845 network supporting perceptually-decoupled and conceptually-guided cognition.
846 *NeuroImage*, 171(January), 393–401.
847 <https://doi.org/10.1016/j.neuroimage.2018.01.017>

848 Murphy, C., Wang, H. T., Konu, D., Lowndes, R., Margulies, D. S., Jefferies, E., & Smallwood, J.
849 (2019). Modes of operation: A topographic neural gradient supporting stimulus
850 dependent and independent cognition. *NeuroImage*, 186(November 2018), 487–496.
851 <https://doi.org/10.1016/j.neuroimage.2018.11.009>

852 Murphy, K., Birn, R. M., Handwerker, D. A., Jones, T. B., & Bandettini, P. A. (2009). The impact
853 of global signal regression on resting state correlations: Are anti-correlated networks
854 introduced? *NeuroImage*, 44(3), 893–905.
855 <https://doi.org/10.1016/j.neuroimage.2008.09.036>

856 Naghavi, H. R., & Nyberg, L. (2005). Common fronto-parietal activity in attention, memory,
857 and consciousness: shared demands on integration?. *Consciousness and*
858 *cognition*, 14(2), 390-425. <https://doi.org/10.1016/j.concog.2004.10.003>

859 Noonan, K. a, Jefferies, E., Corbett, F., & Lambon Ralph, M. a. (2010). Elucidating the nature
860 of deregulated semantic cognition in semantic aphasia: evidence for the roles of
861 prefrontal and temporo-parietal cortices. *Journal of Cognitive Neuroscience*, 22(7),
862 1597–1613. <https://doi.org/10.1162/jocn.2009.21289>

863 Noonan, K. a, Jefferies, E., Visser, M., & Lambon Ralph, M. a. (2013). Going beyond Inferior
864 Prefrontal Involvement in Semantic Control: Evidence for the Additional Contribution of
865 Dorsal Angular Gyrus and Posterior Middle Temporal Cortex. *Journal of Cognitive*
866 *Neuroscience*, 1–10. <https://doi.org/10.1162/jocn>

867 Owen, A. M., McMillan, K. M., Laird, A. R., & Bullmore, E. (2005). N-back working memory
868 paradigm: A meta-analysis of normative functional neuroimaging studies. *Human brain*
869 *mapping*, 25(1), 46-59. <https://doi.org/10.1002/hbm.20131>

870 Patterson, K., Nestor, P. J., & Rogers, T. T. (2007). Where do you know what you know? The
871 representation of semantic knowledge in the human brain. *Nature Reviews*.

872 *Neuroscience*, 8(december), 976–987. <https://doi.org/10.1038/nrn2277>

873 Price, Amy R, Bonner, M. F., Peelle, J. E., & Grossman, M. (2015). Converging evidence for the
874 neuroanatomic basis of combinatorial semantics in the angular gyrus. *The Journal of*
875 *Neuroscience : The Official Journal of the Society for Neuroscience*, 35(7), 3276–3284.
876 <https://doi.org/10.1523/JNEUROSCI.3446-14.2015>

877 Price, Amy Rose, Peelle, J. E., Bonner, M. F., Grossman, M., & Hamilton, R. H. (2016). Causal
878 evidence for a mechanism of semantic integration in the angular Gyrus as revealed by
879 high-definition transcranial direct current stimulation. *Journal of Neuroscience*, 36(13),
880 3829–3838. <https://doi.org/10.1523/JNEUROSCI.3120-15.2016>

881 Pylkkänen, L. (2019). The neural basis of combinatory syntax and semantics. *Science*,
882 366(6461), 62–66. <https://doi.org/10.1126/science.aax0050>

883 Raichle, M. E., MacLeod, A. M., Snyder, A. Z., Powers, W. J., Gusnard, D. A., & Shulman, G. L.
884 (2001). A default mode of brain function. *Proceedings of the National Academy of*
885 *Sciences of the United States of America*, 98(2), 676–682.
886 <https://doi.org/10.1073/pnas.98.2.676>

887 Ramanan, S., Piguët, O., & Irish, M. (2017). Rethinking the Role of the Angular Gyrus in
888 Remembering the Past and Imagining the Future: The Contextual Integration Model. *The*
889 *Neuroscientist*, 107385841773551. <https://doi.org/10.1177/1073858417735514>

890 Robin, J., Buchsbaum, B. R., & Moscovitch, M. (2018). The primacy of spatial context in the
891 neural representation of events. *The Journal of Neuroscience*, 38(11), 1638–17.
892 <https://doi.org/10.1523/JNEUROSCI.1638-17.2018>

893 Rodd, J. M., Cai, Z. G., Betts, H. N., Hanby, B., Hutchinson, C., & Adler, A. (2016). The impact
894 of recent and long-term experience on access to word meanings: Evidence from large-
895 scale internet-based experiments. *Journal of Memory and Language*, 87, 16–37.
896 <https://doi.org/10.1016/j.jml.2015.10.006>

897 Rodd, J. M., Davis, M. H., & Johnsrude, I. S. (2005). The neural mechanisms of speech
898 comprehension: fMRI studies of semantic ambiguity. *Cerebral Cortex*, 15(8), 1261–1269.
899 <https://doi.org/10.1093/cercor/bhi009>

900 Rodd, J. M., Gaskell, M. G., & Marslen-Wilson, W. D. (2004). Modelling the effects of semantic
901 ambiguity in word recognition. *Cognitive Science*, 28(1), 89–104.
902 <https://doi.org/10.1016/j.cogsci.2003.08.002>

903 Rodd, J. M., Lopez Cutrin, B., Kirsch, H., Millar, A., & Davis, M. H. (2013). Long-term priming of
904 the meanings of ambiguous words. *Journal of Memory and Language*, 68(2), 180–198.
905 <https://doi.org/10.1016/j.jml.2012.08.002>

906 Seghier, M. L., Lazeyras, F., Pegna, A. J., Annoni, J. M., Zimine, I., Mayer, E., ... & Khateb, A.
907 (2004). Variability of fMRI activation during a phonological and semantic language task
908 in healthy subjects. *Human brain mapping*, 23(3), 140-155.
909 <https://doi.org/10.1002/hbm.20053>

910 Seghier, M. L., Fagan, E., & Price, C. J. (2010). Functional subdivisions in the left angular gyrus
911 where the semantic system meets and diverges from the default network. *Journal of*
912 *Neuroscience*, 30(50), 16809–16817. <https://doi.org/10.1523/JNEUROSCI.3377-10.2010>

913 Simpson, J. R., Öngür, D., Akbudak, E., Conturo, T. E., Ollinger, J. M., Snyder, A. Z., ... Raichle,
914 M. E. (2000). The emotional modulation of cognitive processing: An fMRI study. *Journal*
915 *of Cognitive Neuroscience*, 12(SUPPL. 2), 157–170.
916 <https://doi.org/10.1162/089892900564019>

917 Smallwood, J. (2013). Distinguishing how from why the mind wanders: A process-occurrence
918 framework for self-generated mental activity. *Psychological Bulletin*, 139(3), 519–535.
919 <https://doi.org/10.1037/a0030010>

920 Smith, S. M. (2002). Fast robust automated brain extraction. *Human Brain Mapping*, 17(3),
921 143–155. <https://doi.org/10.1002/hbm.10062>

922 Teige, C., Cornelissen, P. L., Mollo, G., Gonzalez Alam, T. R. del J., McCarty, K., Smallwood, J.,
923 & Jefferies, E. (2019). Dissociations in semantic cognition: Oscillatory evidence for
924 opposing effects of semantic control and type of semantic relation in anterior and
925 posterior temporal cortex. *Cortex*, 120, 308–325.
926 <https://doi.org/10.1016/j.cortex.2019.07.002>

927 Teige, C., Mollo, G., Millman, R., Savill, N., Smallwood, J., Cornelissen, P. L., & Jefferies, E.
928 (2018). Dynamic semantic cognition: Characterising coherent and controlled conceptual

929 retrieval through time using magnetoencephalography and chronometric transcranial
930 magnetic stimulation. *Cortex*, 103, 329–349.
931 <https://doi.org/10.1016/j.cortex.2018.03.024>

932 Townsend, J. T., & Ashby, F. G. (1983). Stochastic Modeling of Elementary Psychological
933 Processes. *The American Journal of Psychology*, 98(3), 480.
934 <https://doi.org/10.2307/1422636>

935 Twilley, L. C., Dixon, P., Taylor, D., & Clark, K. (1994). University of Alberta norms of relative
936 meaning frequency for 566 homographs. *Memory & Cognition*, 22(1), 111–126.
937 <https://doi.org/10.3758/BF03202766>

938 van Heuven, W. J., Mandera, P., Keuleers, E., & Brysbaert, M. (2014). SUBTLEX-UK: A new and
939 improved word frequency database for British English. *The Quarterly Journal of*
940 *Experimental Psychology*, 67(6), 1176–1190.
941 <https://doi.org/10.1080/17470218.2013.850521>

942 Vatansever, D., Manktelow, A. E., Sahakian, B. J., Menon, D. K., & Stamatakis, E. A. (2017).
943 Angular default mode network connectivity across working memory load. *Human Brain*
944 *Mapping*, 38(1), 41–52. <https://doi.org/10.1002/hbm.23341>

945 Vatansever, Deniz, Menon, X. D. K., Manktelow, A. E., Sahakian, B. J., & Stamatakis, E. A.
946 (2015). Default Mode Dynamics for Global Functional Integration. *The Journal of*
947 *Neuroscience : The Official Journal of the Society for Neuroscience*, 35(46), 15254–
948 15262. <https://doi.org/10.1523/JNEUROSCI.2135-15.2015>

949 Vitello, S., & Rodd, J. M. (2015). Resolving Semantic Ambiguities in Sentences: Cognitive
950 Processes and Brain Mechanisms. *Linguistics and Language Compass*, 9(10), 391–405.
951 <https://doi.org/10.1111/lnc3.12160>

952 Whitfield-Gabrieli, S., & Nieto-Castanon, A. (2012). Conn: A Functional Connectivity Toolbox
953 for Correlated and Anticorrelated Brain Networks. *Brain Connectivity*, 2(3), 125–141.
954 <https://doi.org/10.1089/brain.2012.0073>

955 Whitney, C., Kirk, M., O’Sullivan, J., Lambon Ralph, M. a., & Jefferies, E. (2011). The neural
956 organization of semantic control: TMS evidence for a distributed network in left inferior
957 frontal and posterior middle temporal gyrus. *Cerebral Cortex*, 21(5), 1066–1075.

958 <https://doi.org/10.1093/cercor/bhq180>

959 Willenbockel, V., Sadr, J., Fiset, D., Horne, G. O., Gosselin, F., & Tanaka, J. W. (2010).
960 Controlling low-level image properties: The SHINE toolbox. *Behavior Research Methods*,
961 42(3), 671–684. <https://doi.org/10.3758/BRM.42.3.671>

962 Woolgar, A., Hampshire, A., Thompson, R., & Duncan, J. (2011). Adaptive coding of task-
963 relevant information in human frontoparietal cortex. *Journal of Neuroscience*, 31(41),
964 14592–14599. <https://doi.org/10.1523/JNEUROSCI.2616-11.2011>

965 Woolrich, M. (2008). Robust group analysis using outlier inference. *NeuroImage*, 41(2), 286–
966 301. <https://doi.org/10.1016/j.neuroimage.2008.02.042>

967 Woolrich, M. W., Behrens, T. E. J., Beckmann, C. F., Jenkinson, M., & Smith, S. M. (2004).
968 Multilevel linear modelling for fMRI group analysis using Bayesian inference.
969 *NeuroImage*, 21(4), 1732–1747. <https://doi.org/10.1016/j.neuroimage.2003.12.023>

970 Woolrich, M. W., Ripley, B. D., Brady, M., & Smith, S. M. (2001). Temporal autocorrelation in
971 univariate linear modeling of fMRI data. *NeuroImage*, 14(6), 1370–1386.
972 <https://doi.org/10.1006/nimg.2001.0931>

973 Worsley, K.J. Statistical analysis of activation images. Ch 14, in *Functional MRI: An*
974 *Introduction to Methods*, eds. P. Jefferies, P.M. Matthews and S.M. Smith. OUP, 2001.

975 Xia, M., Wang, J., & He, Y. (2013). BrainNet Viewer: A Network Visualization Tool for Human
976 Brain Connectomics. *PLoS ONE*, 8(7). <https://doi.org/10.1371/journal.pone.0068910>

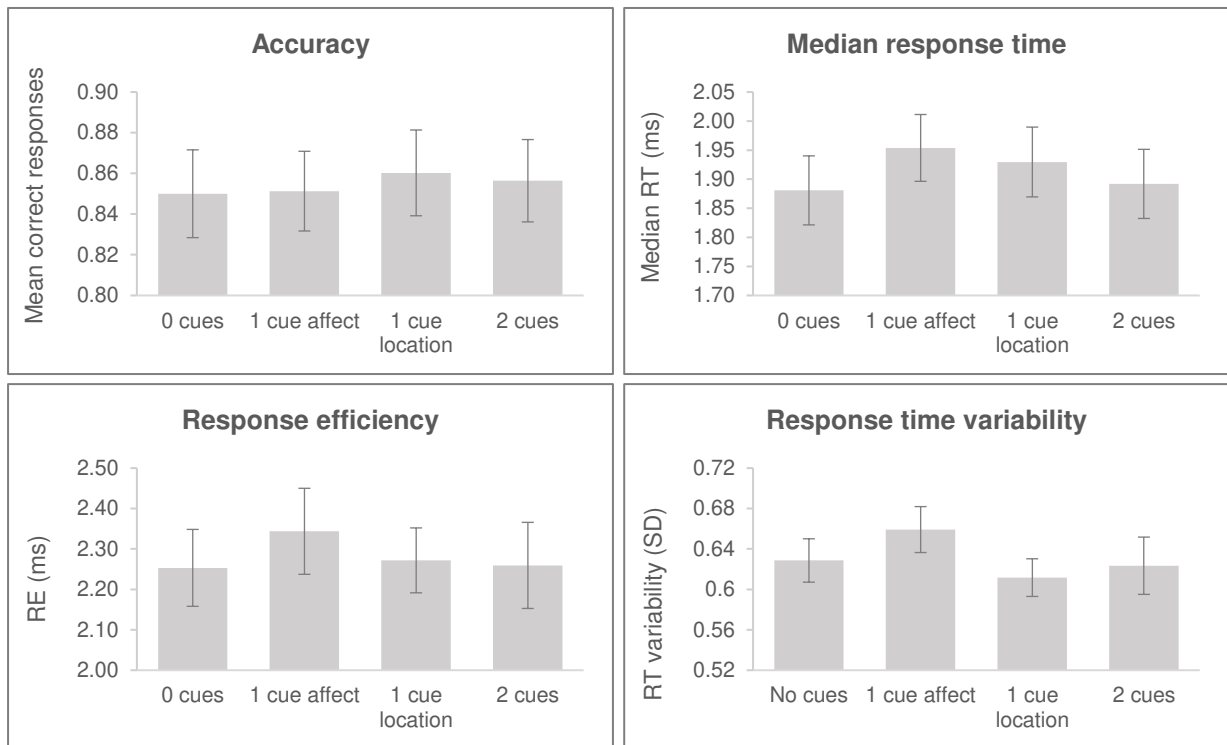
977 Yarkoni, T., Poldrack, R. A., Nichols, T. E., Van Essen, D. C., & Wager, T. D. (2011). Large-scale
978 automated synthesis of human functional neuroimaging data. *Nature Methods*, 8(8),
979 665–670. <https://doi.org/10.1038/nmeth.1635>

980 Yeo, B. T. T., Krienen, F. M., Sepulcre, J., Sabuncu, M. R., Lashkari, D., Hollinshead, M., ...
981 Buckner, R. L. (2011). The organization of the human cerebral cortex estimated by
982 intrinsic functional connectivity. *Journal of Neurophysiology*, 106, 1125–1165.
983 <https://doi.org/10.1152/jn.00338.2011>.

984

985 SUPPLEMENTARY MATERIAL

986 Group behavioural performance



987

988 Figure S1. Accuracy (mean correct responses), median RT for correct trials (milliseconds), response efficiency
 989 scores (median RT/mean correct responses), and RT variability (mean standard deviation per participant per
 990 condition) do not differ significantly across conditions. Error bars show standard error of the mean (SEM).

991

Summary statistics

	Accuracy	Median RT	Response efficiency	RT variability
0 cues	0.85 (0.11)	1.88 (0.30)	2.25 (0.49)	0.63 (0.11)
1 cue affect	0.85 (0.10)	1.95 (0.29)	2.34 (0.54)	0.66 (0.12)
1 cue location	0.86 (0.11)	1.93 (0.31)	2.27 (0.41)	0.61 (0.10)
2 cues	0.86 (0.10)	1.89 (0.30)	2.26 (0.54)	0.62 (0.14)

992

993 Table S1. Descriptive statistics for the cueing task. Mean and (standard deviation) values are provided.

994

995

996 Supplementary behavioural analyses

1- way repeated measures ANOVAs on cue condition

	Accuracy	Median RT	Response efficiency	RT variability
F	0.14	0.95	0.62	1.26
df	3, 75	3, 75	3, 75	3, 75
p	0.939	0.420	0.605	0.296
partial η^2	0.01	0.04	0.02	0.05

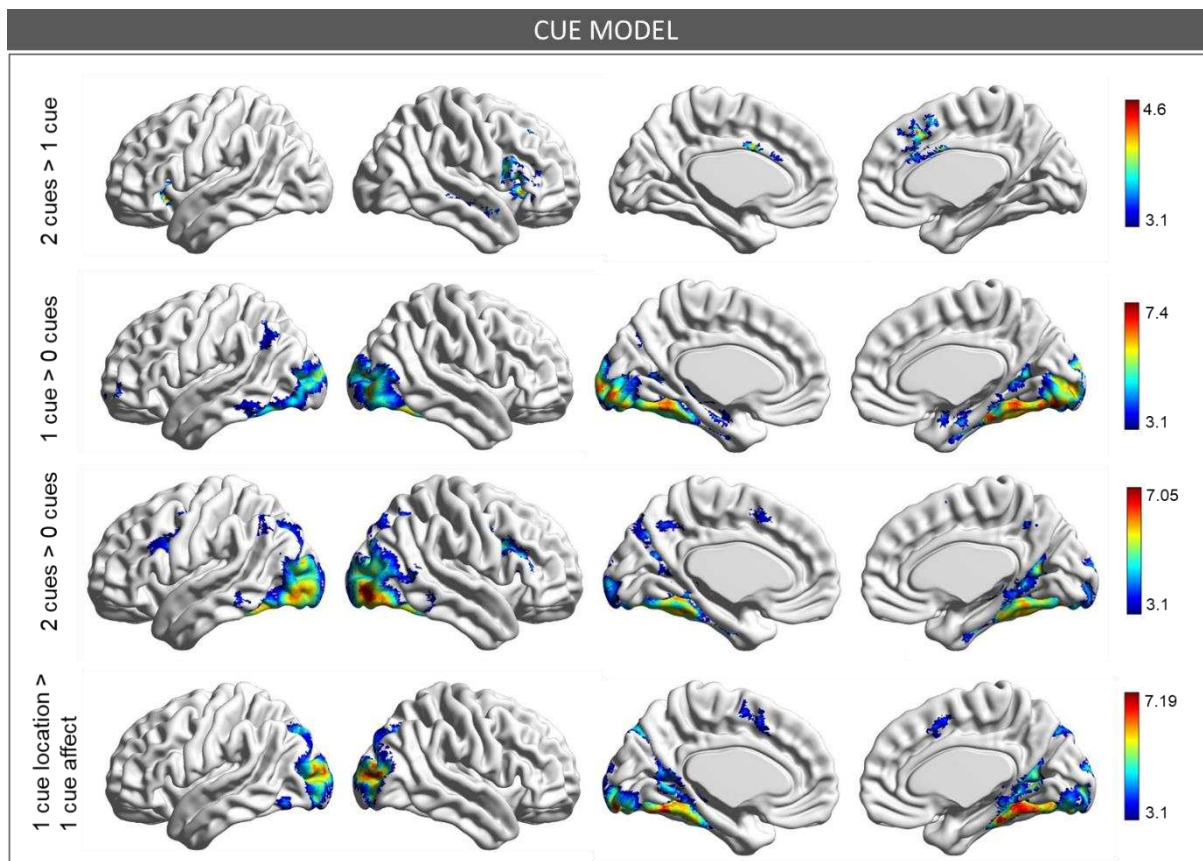
997

998 Table S2. Behavioural performance did not differ significantly across cue conditions, as revealed by 1-way ANOVAs
999 on accuracy, median response time, response efficiency, and response time variability.

1000

1001 Univariate contrasts of activation during cue presentation

1002 Below we report the group-level statistical maps ($z > 3.1$) for the cue model. In this model we
1003 looked at changes in the BOLD response in response to the presentation of the visual cues.
1004 Semantic decisions (which happen subsequently to the presentation of cues) were modelled
1005 separately; the statistical maps that survived the threshold of $z > 3.1$ can be seen in the body
1006 of the manuscript (Figure 2B and 4).

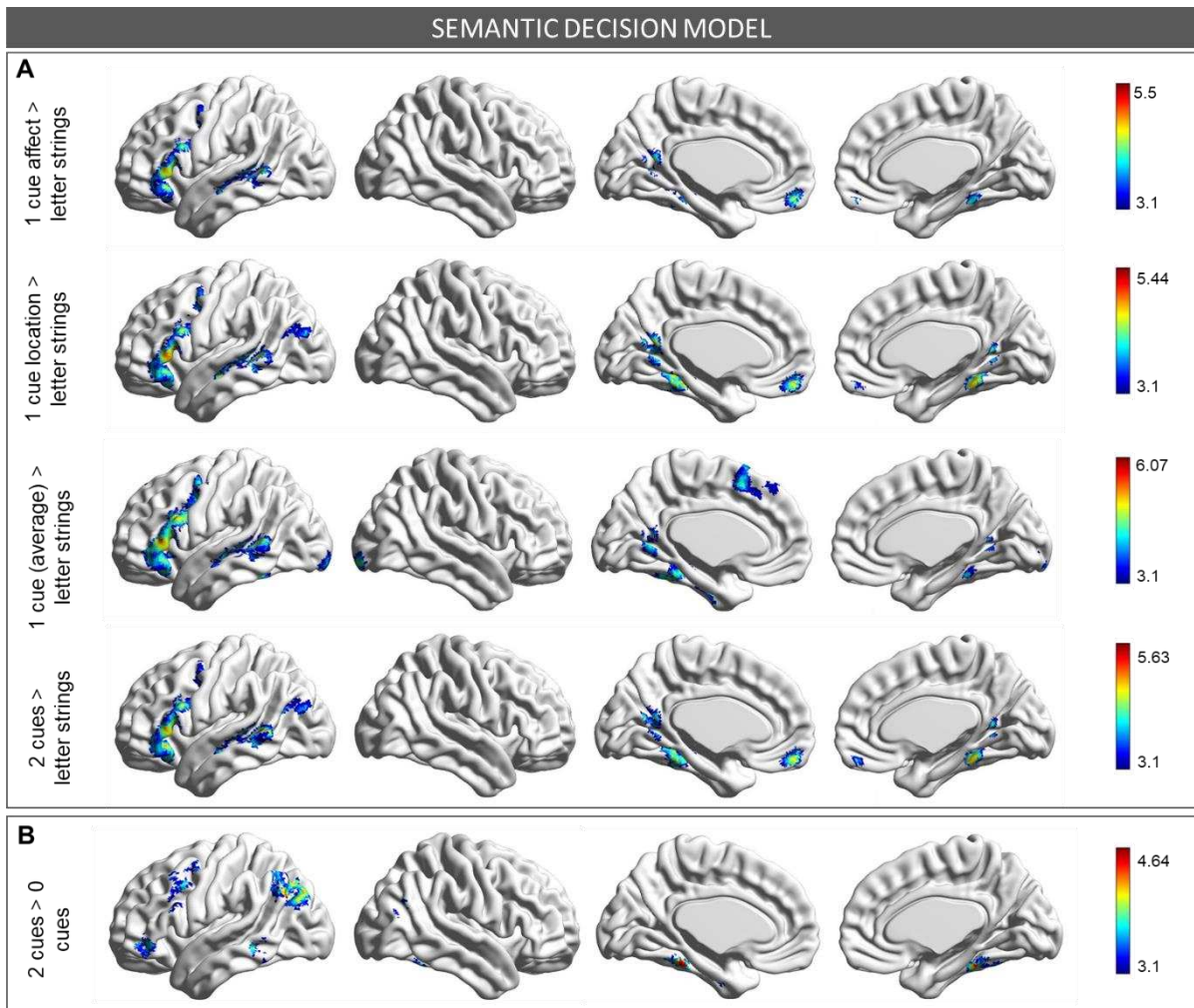


1007

1008 Figure S2. Univariate results for the cue model (i.e. when the cues were presented, prior to the semantic decision).
 1009 From top to bottom: 2 cues > 1 cue (processing of 2 cues > 1 cue [average of affect and location]), 1 cue > 0 cues
 1010 (processing of 1 cue [average of affect and location] > 0 cues [scrambled images]); 2 cues > 0 cues; 1 cue location
 1011 > 1 cue affect. The reverse contrast (1 cue affect > 1 cue location) yielded no clusters. Coordinates of cluster peaks
 1012 for these comparisons are reported in Table S3.

1013 Basic effect of semantic decisions

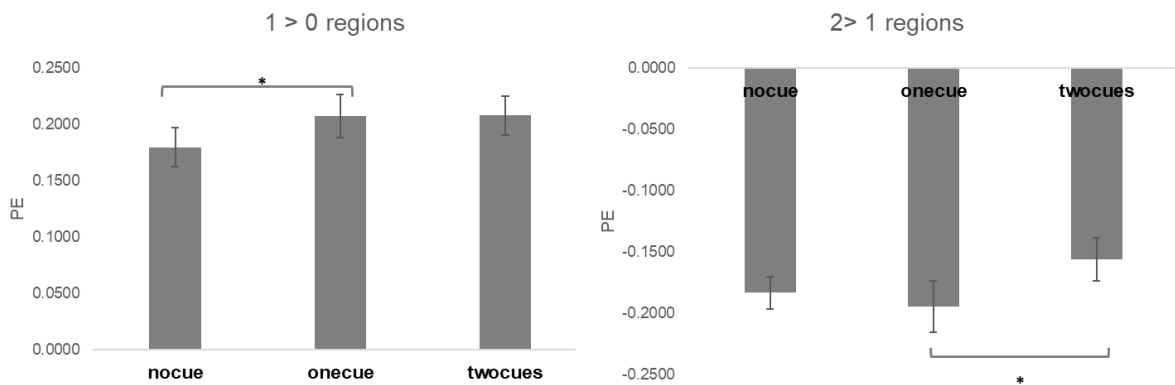
1014 In the main manuscript we defined the semantic regions recruited during the task using a
 1015 contrast of 0 cues > letter strings (Figure 2A). Below we report the contrasts of each of the
 1016 other task conditions against the presentation of letter strings (i.e. non semantic task).



1017

1018 Figure S3. A. Basic effect of semantic decisions as estimated by contrasts of the task conditions > letter strings
 1019 (i.e. non-semantic task). These univariate contrasts for the semantic decision model (i.e. when participants were
 1020 making decisions following the presentation of 0, 1, 2 cues) reveal a similar pattern of activation. B. Semantic
 1021 decisions following 2 cues vs. 0 cues.

1022



1023

1024 Figure S4. ROI analysis extracting the parameter estimates (PE) for the three conditions over the implicit baseline
 1025 at the time of making semantic decisions (semantic decision model) in the 1 > 0 and 2 > 1 maps. We ran two
 1026 repeated measures ANOVAs that found that the recruitment is different across cueing conditions in both 1 > 0 [F
 1027 (2,50) = 3.36, p = .043, $\eta^2 = .12$] and 2 > 1 [F (2,50) = 3.47, p = .039, $\eta^2 = .12$] regions. Bonferroni-corrected pairwise
 1028 comparisons revealed reduced activation for 0 cue condition compared to 1 cue in 1 > 0 regions [t(25) = -2.59, p
 1029 = .016], and reduced de-activation in 2 cues compared to 1 cue in 2 > 1 regions [t(25) = -3.03, p = .006].

1030 Peak co-ordinates for clusters identified by the cue model and the semantic decision model

Contrast	Region	Voxels	Z-score	MNI coordinates (x, y, z)		
<i>Cue model</i>						
2 + 1 > 0	R. Lingual gyrus, occipital fusiform gyrus, occipital pole	26628	7.49	8	-82	-12
	L. Middle frontal gyrus, superior frontal gyrus	769	4.51	-36	22	54
	L. Frontal pole	766	4.99	-42	54	-4
	L. temporal pole, inferior temporal gyrus (anterior), temporal fusiform gyrus (anterior)	130	4.29	-42	4	-42
2 > 0	R. Lateral occipital cortex (inferior), occipital pole	21099	7.05	42	-86	-8
	R. Precentral gyrus, inferior frontal gyrus, middle frontal gyrus	866	5.11	38	10	28
	L. Inferior frontal gyrus (pars opercularis), precentral gyrus, middle frontal gyrus	850	4.63	-40	16	22
	Bilateral precuneus	189	4.11	0	-56	46
	L. Supplementary motor cortex, paracingulate gyrus, superior frontal gyrus	177	4.29	-4	6	54
2 > 1	R. Frontal operculum cortex, inferior frontal gyrus (pars opercularis), inferior frontal gyrus (pars triangularis)	940	4.48	46	18	6
	R. Paracingulate gyrus, superior frontal gyrus, cingulate gyrus (anterior)	585	4.38	6	24	44
	R. Middle frontal gyrus, superior frontal gyrus, frontal pole	267	4.55	28	32	44
	R. Superior temporal gyrus (anterior), middle temporal gyrus (anterior), superior temporal gyrus (posterior), middle temporal gyrus (posterior)	199	4.35	54	-6	-16
	L. Insular cortex	152	4.51	-28	20	-6
1 > 0	R. Occipital fusiform gyrus, lingual gyrus	21130	7.38	24	-72	-14
	L. Lateral occipital cortex (superior), angular gyrus	229	4	-50	-66	40
	L. Frontal pole	229	4.51	-40	58	2
	R. Cerebellum	198	4.24	28	-74	-44
1 location > 1 affect	R. Occipital pole, lateral occipital cortex	17891	7.19	36	-88	8
	Bilateral paracingulate gyrus, supplementary motor cortex	411	4.31	0	10	50
<i>Semantic decision model</i>						
0 > letter strings	L. Inferior frontal gyrus (pars triangularis), frontal pole, middle frontal gyrus	1672	5.92	-54	32	8

	L. Superior temporal gyrus (posterior), middle temporal gyrus (posterior), supramarginal gyrus (posterior)	953	5.52	-56	-42	4
	R. Cerebellum	644	5.04	10	-82	-36
	L. Temporal fusiform cortex (posterior), parahippocampal gyrus (posterior), inferior temporal gyrus (posterior)	400	4.51	-38	-30	-18
	L. Cerebellum	280	4.62	-8	-60	14
	L. Frontal medial cortex, frontal pole	256	4.66	-4	52	-16
	R. Temporal occipital fusiform, Lingual gyrus, parahippocampal gyrus (posterior)	220	4.91	22	-42	-16
	L. Precentral gyrus, middle frontal gyrus	153	4.7	-38	0	46
	L. Inferior frontal gyrus (pars triangularis), frontal pole, middle frontal gyrus	1684	4.91	-56	32	6
	L. Middle temporal gyrus (temporo-occipital part), middle temporal gyrus (posterior)	926	5.5	-56	-44	4
	R. Cerebellum	571	4.81	10	-82	-36
1 affect > letter strings	L. Temporal fusiform (posterior), parahippocampal gyrus (posterior), inferior temporal gyrus (posterior)	261	4.2	-38	-30	-18
	L. Precuneus, intracalcarine cortex, supracalcarine cortex, cingulate gyrus (posterior)	258	4.65	-8	-60	14
	L. Medial frontal cortex, frontal pole	186	4.6	-2	52	-16
	R. Temporal fusiform (posterior), parahippocampal gyrus (posterior), lingual gyrus	138	4.19	24	-38	-18
	L. Precentral gyrus, middle frontal gyrus	125	4.11	-38	0	44
	L. Inferior frontal gyrus (pars triangularis), frontal pole, middle frontal gyrus	2000	5.44	-56	32	8
	L. Middle temporal gyrus (temporo-occipital part), middle temporal gyrus (posterior)	1107	5.04	-58	-44	4
	R. Cerebellum	910	5.12	12	-78	-30
1 location > letter strings	L. Temporal fusiform (posterior), parahippocampal gyrus (posterior), inferior temporal gyrus (posterior)	773	5.06	-38	-30	-18
	L. Precuneus, intracalcarine cortex, lingual gyrus, supracalcarine cortex, cingulate gyrus (posterior)	723	4.93	-8	-60	10
	R. Lingual gyrus, occipital fusiform gyrus, parahippocampal gyrus (posterior), temporal fusiform (posterior)	375	5.4	20	-40	-16
	L. Medial frontal cortex, frontal pole	230	4.71	-2	52	-16
	L. Precentral gyrus, middle frontal gyrus	205	4.61	-38	0	44
	L. Lateral occipital cortex (superior)	176	3.97	-44	-84	26
	L. Inferior frontal gyrus (pars triangularis), frontal pole, middle frontal gyrus	3459	5.65	-54	30	8
	L. Middle temporal gyrus (temporo-occipital part), middle temporal gyrus (posterior)	2493	5.41	-56	-44	4
1 > letter strings	R. Cerebellum	1165	6.07	12	-78	-28
	L. Precuneus, lingual gyrus, intracalcarine cortex, cingulate gyrus (posterior), supracalcarine cortex	371	4.73	-6	-58	8
	L. Paracingulate gyrus, superior frontal gyrus, juxtapositional lobule	337	4.56	-6	14	52
	R. Occipital pole	275	4.89	18	100	-12

	L. Occipital pole	235	4.91	-34	-98	-14
	R. Precuneus, lingual gyrus, intracalcarine cortex, cingulate gyrus (posterior), supracalcarine cortex	127	4.54	14	-56	6
	R. temporal fusiform (posterior), parahippocampal gyrus (posterior), lingual gyrus	118	4.37	28	-36	-20
	L. Inferior frontal gyrus (pars triangularis), frontal pole, middle frontal gyrus	2239	5.51	-56	32	8
	L. Middle temporal gyrus (temporo-occipital), middle temporal gyrus (posterior), supra-marginal gyrus (posterior), , superior temporal gyrus (posterior)	1175	5.63	-48	-44	-2
	R. Cerebellum	794	4.79	10	-82	-34
	L. Temporal fusiform (posterior), temporal occipital fusiform, parahippocampal gyrus (posterior), lingual gyrus	695	4.95	-26	-42	-20
2 > letter strings	L. Precuneus, lingual gyrus, intracalcarine cortex, cingulate gyrus (posterior), supracalcarine cortex	458	4.77	-8	-58	10
	R. Temporal occipital fusiform, Lingual gyrus, temporal fusiform (posterior), parahippocampal gyrus (posterior)	367	5.6	22	-40	-16
	L. Angular gyrus, lateral occipital cortex (superior), lateral occipital cortex (inferior)	265	4.4	-40	-60	18
	L. Frontal medial cortex, frontal pole	237	4.82	-2	52	-16
	R. Precuneus, Intracalcarine cortex, cingulate gyrus (posterior), lingual gyrus, supracalcarine cortex	201	4.67	16	-54	8
	R. Lateral occipital cortex (superior)	5247	5.94	52	-70	30
	R. Frontal pole, paracingulate gyrus, frontal medial cortex	4395	5.57	4	56	0
2 > 1	L. lateral occipital cortex (superior), angular gyrus, supramarginal gyrus (posterior)	1639	5.27	-50	-62	42
	R. Precuneus, cingulate gyrus (posterior)	1521	5.17	8	-56	26
	L. Cerebellum	745	4.77	-26	-78	-36
	L. Middle frontal gyrus	304	4.46	-36	26	42
	R. Frontal pole	191	4.35	40	48	-10
	L. Frontal pole	172	4.33	-30	62	-2
	R. Temporo-occipital fusiform, lingual gyrus, parahippocampal gyrus	143	4.72	24	-42	-16
	R. Cerebellum	30503	6.81	4	-74	-28
	L. Supplementary motor cortex, paracingulate gyrus, superior frontal gyrus, cingulate gyrus (anterior)	2167	6.57	-4	8	52
1 > 0	R. Inferior frontal gyrus (pars opercularis), middle frontal gyrus, inferior frontal gyrus (pars triangularis), precentral gyrus	714	5.59	42	22	20
	L. Middle temporal gyrus (temporo-occipital), supra-marginal gyrus (posterior), middle temporal gyrus (posterior), superior temporal gyrus	254	4.85	-56	-46	4
	L. Lateral occipital cortex (superior), angular gyrus	1431	4.55	-46	-66	32
2 > 0	R. Lateral occipital cortex (inferior), occipital fusiform gyrus	533	4.55	38	-74	-24
	L. Middle frontal gyrus, precentral gyrus, inferior frontal gyrus (pars opercularis)	472	4.04	-46	12	40

L. Temporal fusiform cortex (posterior), temporal occipital fusiform cortex, parahippocampal gyrus (posterior)	441	4.64	-26	-40	-20
L. Occipital fusiform gyrus	283	4.55	-46	-72	-26
L. Frontal pole, frontal orbital cortex, inferior frontal gyrus (pars triangularis)	153	3.94	-52	40	-8
L. Middle temporal gyrus (posterior), middle temporal gyrus (temporooccipital)	128	3.97	-60	-40	-8
R. Lateral occipital cortex (superior), angular gyrus	125	3.94	52	-64	24

1031

1032 Table S3. Coordinates of cluster peaks for the main contrasts of interest. From top to bottom: cue model – 2 + 1
1033 > 0 (processing of cues > scrambles images), 2 > 0 (processing of 2 cues [affect and location] > 0 cues [scrambled
1034 images]), 2 > 1 (processing of 2 cues [affect and location] > 1 cue [average of affect and location]), 1 > 0
1035 (processing of 1 cue [average of affect and location] > 0 cues [scrambled images]), 1 affect > 1 location; semantic
1036 decision model - 0 cues > letter strings (semantic decisions in the absence of a semantic cue > non semantic
1037 decisions in the absence of cues), 1 affect > letter strings, 1 location > letter strings, 1 > letter strings (semantic
1038 decision following 1 cue [average of affect and location] > non semantic decisions in the absence of cues), 2 >
1039 letter strings, 2 > 1 (semantic decisions following multiple cues > semantic decisions following 1 cue), 1 > 0
1040 (semantic decisions following 1 semantic cue > semantic decisions in the absence of a semantic cue). The location
1041 of the peaks is labelled according to the Harvard-Oxford Structural Cortical Atlas tool available in FSL. Caption: R
1042 = right hemisphere, L = left hemisphere, cluster corrected at $z > 3.1$.

1043

1044

1045

1046 Supplementary analyses examining activation for the semantic task along the Principal
 1047 Gradient

2 (cue contrast: 2 vs. 1, 1 vs. 0) x 10 (gradient bin: bin1 - bin10) ANOVA

	Test of within-subjects effect			Test of within-subjects contrasts			
	Cue contrast	Gradient bin	Cue contrast x gradient bin	Cue contrast	Gradient bin	Cue contrast x gradient bin	
F	0.33	1.82	28.33	0.33	1.53	37.27	Linear
p	.571	.164	<.001*	.571	.227	<.001*	
partial η^2	0.01	0.07	0.53	0.01	0.06	0.60	
F					0.06	12.37	Quadratic
p					.815	.002*	
partial η^2					0.00	0.33	
F					2.26	6.47	Cubic
p					.145	.018*	
partial η^2					0.08	0.21	
F					0.79	0.28	Order 4
p					.382	.601	
partial η^2					0.03	0.01	
F					20.44	111.60	Order 5
p					<.001*	<.001*	
partial η^2					0.45	0.82	
F					1.06	9.51	Order 6
p					.312	.005*	
partial η^2					0.04	0.28	
F					5.07	38.85	Order 7
p					.033*	<.001*	
partial η^2					0.17	0.61	
F					2.50	64.54	Order 8
p					.127	<.001*	
partial η^2					0.09	0.72	
F					1.07	66.73	Order 9
p					.311	<.001*	
partial η^2					0.04	0.73	

1048

1049 Table S4. Values for the 2-way repeated measure ANOVA on cue contrast (2 levels: 2 cues > 1 cue; 1 cue > 0 cues)
 1050 and gradient bin (10 levels: bin1 – bin10). Degrees of freedom for the Test of Within-subjects Effects: cue
 1051 condition [1, 25]; gradient bin [2.37, 59.16]; cue contrast x gradient bin [2.04, 51.01]. Degrees of freedom for the
 1052 Test of Within-subjects Contrasts: cue contrast, gradient bin, cue contrast x gradient bin [1, 25]. Significant results
 1053 and interactions are marked with *. A Greenhouse-Geisser correction was applied where the assumption of
 1054 sphericity was not met.

1055

1 way RM ANOVA on 2 cues > 1 cue along the gradient			
	Test of within-subjects effect	Test of within-subjects contrasts	
	Gradient bin	Gradient bin	
F	31.50	47.13	Linear
p	<.001*	<.001*	
partial η^2	0.56	0.65	
F		11.38	Quadratic
p		.002*	
partial η^2		0.31	
F		3.03	Cubic
p		.094	
partial η^2		0.11	
F		0.06	Order 4
p		.813	
partial η^2		0.00	
F		70.22	Order 5
p		<.001*	
partial η^2		0.74	
F		7.66	Order 6
p		.010*	
partial η^2		0.23	
F		31.30	Order 7
p		<.001*	
partial η^2		0.56	
F		48.60	Order 8
p		<.001*	
partial η^2		0.66	
F		50.58	Order 9
p		<.001*	
partial η^2		0.67	

1056

1057 Table S5. Values for the 1-way repeated measure ANOVA on the parameter estimates for the univariate contrast
 1058 of 2 cues > 1 cue extracted along the gradient (10 levels: bin1 – bin10). Degrees of freedom for the Test of Within-
 1059 subjects Effects: 2.13, 53.30. Degrees of freedom for the Test of Within-subjects Contrasts: 1, 25. Significant
 1060 results and interactions are marked with *. A Greenhouse-Geisser correction was applied where the assumption
 1061 of sphericity was not met.

1062

1063

1064

1 way RM ANOVA on 1 cue > 0 cues along the gradient			
	Test of within-subjects effect	Test of within-subjects contrasts	
	Gradient bin	Gradient bin	
F	21.37	24.80	Linear
p	<.001*	<.001*	
partial η^2	0.46	0.50	
F		11.48	Quadratic
p		.002*	
partial η^2		0.31	
F		7.44	Cubic
p		.011*	
partial η^2		0.23	
F		0.52	Order 4
p		.478	
partial η^2		0.02	
F		116.31	Order 5
p		<.001*	
partial η^2		0.82	
F		8.61	Order 6
p		.007*	
partial η^2		0.26	
F		40.27	Order 7
p		<.001*	
partial η^2		0.62	
F		62.44	Order 8
p		<.001*	
partial η^2		0.71	
F		64.32	Order 9
p		<.001*	
partial η^2		0.72	

1065

1066 Table S6. Values for the 1-way repeated measure ANOVA on the parameter estimates for the univariate contrast
 1067 of 1 cue > 0 cues extracted along the gradient (10 levels: bin1 – bin10). Degrees of freedom for the Test of Within-
 1068 subjects Effects: 2.05, 51.22. Degrees of freedom for the Test of Within-subjects Contrasts: 1, 25. Significant
 1069 results and interactions are marked with *. A Greenhouse-Geisser correction was applied where the assumption
 1070 of sphericity was not met.

1071

1072

1073

1074 **Analysis of intrinsic connectivity**

1075 As there is evidence that DMN is anti-correlated with task-positive regions captured by MDN
1076 (Blank et al., 2014; Davey et al., 2016; Fox et al., 2005), we predicted that our contrast maps
1077 of $1 > 0$ and $2 > 1$ should fall within regions with distinct patterns of intrinsic connectivity at rest,
1078 given their spatial similarity with the MDN and with the DMN, respectively.

1079 ***Materials and Methods***

1080 *Participants*

1081 Whole-brain intrinsic connectivity maps for the two contrasts ($1 > 0$ and $2 > 1$) were produced
1082 using a sample of 86 participants recruited as part of a different study. The study was approved
1083 by the Ethics Committees of the York Neuroimaging Centre and the Department of Psychology,
1084 University of York. Volunteers provided written consent and were debriefed after the
1085 experiment.

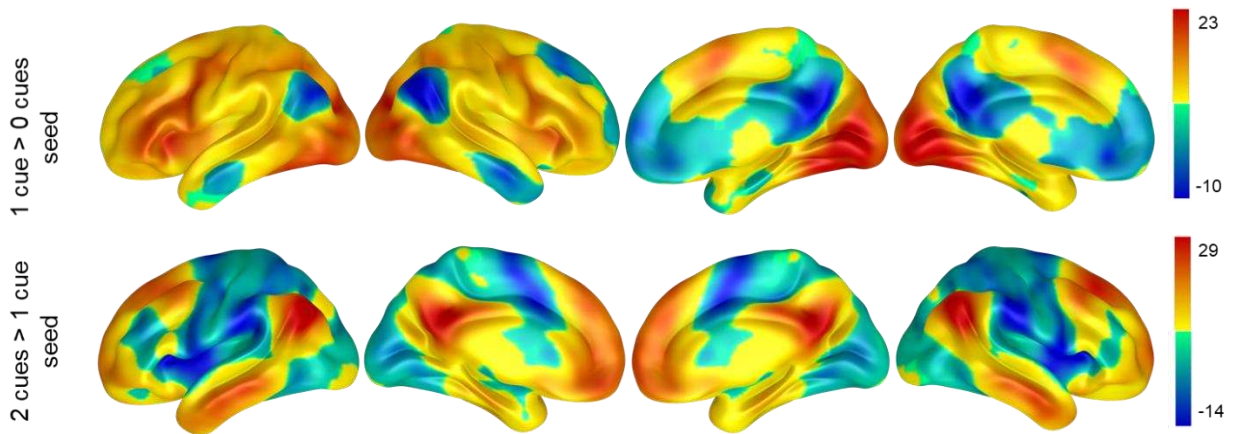
1086 *MRI data acquisition*

1087 Structural and functional MRI data were acquired using a 3T GE HDx Excite MRI scanner at the
1088 York Neuroimaging Centre, University of York. Structural MRI acquisition was based on the
1089 same protocol used for the main sample of this experiment (see Materials and Methods—*fMRI*
1090 *acquisition*). Resting-state fMRI data was recorded from the whole brain using single-shot 2D
1091 gradient-echo-planar imaging (TR=3s, TE=minimum full, flip angle=90°, matrix size=64x64, 60
1092 slices, voxel size=3x3x3mm³, 180 volumes). Participants were asked to passively view a fixation
1093 cross and not to think of anything in particular for the duration of the resting-state scan (9
1094 minutes). A T1 weighted FLAIR scan with the same orientation as the functional scans was
1095 collected to improve co-registration between subject-specific structural and functional scans
1096 (TR=2560ms, TE=minimum full, matrix size=64x64, voxel size=3x3x3mm³).

1097 *Pre-processing*

1098 The pre-processing of resting state data was performed using the CONN functional connectivity
1099 toolbox V.18a (<http://www.nitrc.org/projects/conn>; Whitfield-Gabrieli & Nieto-Castanon,
1100 2012). The following steps were performed on the functional volumes: (1) slice-time (bottom-
1101 up, interleaved) and motion-correction, (2) skull-stripping and co-registration to the high-
1102 resolution structural image, (3) spatial normalisation to Montreal Neurological Institute (MNI)

1103 space using the unified-segmentation algorithm, (4) smoothing with a 6mm FWHM Gaussian
1104 kernel, and (5) band-passed filtering (0.008-0.09Hz) to reduce low-frequency drift and noise
1105 effects. Nuisance regressors in the pre-processing pipeline included: (i) motion (12 parameters:
1106 the six translation and rotation parameters and their temporal derivatives), (ii) scrubbing
1107 (outliers were identified through the artefact detection algorithm included in CONN based on
1108 scan-by-scan change in global signal above $z=3$, subject motion threshold above 5mm,
1109 differential motion and composite motion exceeding 95% percentile in the normative sample),
1110 (iii) CompCor components (the first 5) attributable to the signal from white matter and CSF
1111 (Behzadi et al., 2007), and (iv) a linear detrending term, eliminating the need for global signal
1112 normalisation (Chai et al., 2012; Murphy et al., 2009).



1113
1114 Figure S5. Intrinsic connectivity maps obtained in a separate sample of 86 participants using the thresholded ($z >$
1115 3.1) contrast maps of 2 cues > 1cue and 1 cue > 0 as seeds in a resting state analysis. These reveal two functionally
1116 distinct and anti-correlated networks, comprising multiple demand regions for 1>0 and default mode regions for
1117 2>1.

1118

1119